Evidence for the Down-Regulation of *ATP6V1H* Gene Expression in Type 2 Diabetes

Presented by Melanie Molina
In partial fulfillment of the requirements for graduation with the Dean's Scholars Honors Degree in Biology

Under the supervision of Dr. Hui-Qi Qu,
Assistant Professor, Division of Epidemiology, Human Genetics and Environmental Sciences
The University of Texas School of Public Health, Brownsville Regional Campus

_____ _____
Leanne H. Field, Ph.D. Date
Supervising Professor

_____ _____
Arturo De Lozanne, Ph.D. Date
Honors Advisor in Biology

I grant the Dean's Scholars Program permission to (check all that apply):

_____Post a copy of my thesis on the Dean's Scholars website.

_____Keep a copy of my thesis in the Dean's Scholars office for Dean's Scholars to read my Down-Regulation of *ATP6V1H* Gene Expression in Type 2 Diabetes.

Department: Biology

_____
Melanie Molina

_____ _____
Signature Date

_____
Leanne H. Field, Ph.D.

_____ _____
Signature Date

TABLE OF CONTENTS **PAGE**

Type 2 Diabetes: An Alarming Disease in Mexican-Americans

Melanie F. Molina

The University of Texas at Austin, School of Biological Sciences

¡*Atención compadres*! There's a new villain in town.

It's a disease doctors are still trying to pin down.

Type 2 Diabetes, perhaps it's hard to believe,

But hear it now, before turning to leave!

Diabetes targets everyone; all sizes and races.

Its development, however, has partly a genetic basis.

Although Mexicans may not be at the greatest hereditary disadvantage,

Delicious food and lack of exercise make the disease in their culture especially hard to manage.

While scientists search frantically to pinpoint the genes,

It's important that *latinos* make it a routine,

To resist the temptations of *pastels* and sweets,

And be physically active, in spite of the heat.

For if not, this epidemic will be quite hard to delay,

And as for finding a cure, there will simply be no way.

http://blogs.bmj.com/jmg/2011/06/17/type-2-diabetes-an-alarming-disease-in-mexican-americans/

ACKNOWLEDGEMENTS

Before delving into the details of my work in Brownsville, I would first like to let it be known that this project was one of the most challenging yet fruitful endeavors on which I have ever embarked. I gained an immense amount of knowledge and learned how to implement it toward independent and innovative ideas. I have emerged not only with a stronger understanding of laboratory science and clinical research, but also a reinforced passion for public health.

That being said, this work would not have been possible without the help of many people, all of who are deserving of the utmost recognition. I would first like to thank Dr. Susan Fisher-Hoch and Dr. Joseph McCormick. Dr. Fisher-Hoch kindly gave me the opportunity to work in Brownsville and ensured that I was able to pair with a project that met my interests, and Dr. McCormick was always around to make sure my experience went smoothly, giving me words of encouragement every step of the way.

I would also like to thank Dr. Huiqi Qu and his wife, Yang Lu, for having an immense amount of patience with me both in and out of the lab. Dr. Qu was always willing to meet with me if I had any questions, no matter how busy he was, and was even able to collaborate with me on a publication. Yang helped guide me through unfamiliar techniques in the lab—her passion and enthusiasm for science always evident in the way she spoke about the research process. I admire both of them greatly.

I'd also like to thank the cohort recruitment team, particularly Rocio Uribe, Elizabeth Braunstein and Julie Ramirez, as well as Marcela Montemayor and other laboratory staff for their contribution, in addition to Gloria Sanchez for database management and Christina Villarreal for administrative support. I owe thanks to the

Valley Baptist Medical Center, Brownsville for providing space for the Center for Clinical and Translational Science Clinical Research Unit, as well as to the community of Brownsville and the participants who so willingly participated in this study. This work was supported by MD000170 P20 funded from the National Center on Minority Health and Health disparities (NCMHD), and the Centers for Clinical and Translational Science Award from the National Center for Research Resources (NCRR).

Finally, I would like to give special thanks to Dr. Leanne Field. Were it not for her, I would never have obtained the opportunity to work in Brownsville, nor would I have understood how paramount the field of public health has become. She always puts an immense amount of time and effort into ensuring that her students receive the most out of any opportunity they are given and, as a student of hers, I was no exception. She will forever stand in my memory as one of the most influential people in my life.

ABSTRACT

According to the World Health Organization, there are approximately 346 million cases of diabetes worldwide, 90% of which are accredited specifically to type 2 diabetes. As type 2 diabetes continues to raise concern, researchers are beginning to turn their focus to the inherent factors that predispose individuals to the disease, one of which is genetics. Recently, a higher prevalence of type 2 diabetes was observed in a 2,500-member cohort of Mexican-Americans established on the US-Mexican border, specifically in Brownsville (Cameron County), Texas.

The purpose of this research was threefold: 1) to study the demographic and physiological parameters of nine individuals in the CCHC who developed diabetes over the three years of the study period; 2) to investigate whether the gene encoding subunit H of V-ATPase (*ATP6V1H*) was down-regulated in the nine individuals as they progressed from pre-diabetes to type 2 diabetes; 3) to perform an extensive literature review of the *ATP6V1H* gene and its protein product, V-ATPase subunit H, to postulate what role it might play in the development of diabetes and its complications.

Of the nine participants that developed type 2 diabetes, six were female and three were male (ages ranged from 38-81). Six different physiological parameters were measured in each individual at the time of their first and last visits to the clinic: triglyceride, cholesterol, high-density lipoprotein (HDL) cholesterol, low-density lipoprotein (LDL) cholesterol, glucose and HbA1c. Higher levels of triglyceride, HDL cholesterol and glucose were found in the 9 individuals as they progressed from pre-diabetes to type 2 diabetes. These differences were statistically significant. There were no statistically significant differences in any of the other measured parameters. The

gene expression of *ATP6V1H* was assayed using microarray techniques and a paired Z test revealed a statistically significant decrease (p-value = 7.18×10^{-11}) in expression in all nine participants.

Based on the results of this study and an extensive review of the literature, the author hypothesizes that the down-regulated expression of the V-ATPase subunit H protein product may contribute to diabetes and its complications by disrupting the crucial endosomal acidification process necessary for the dissociation of insulin from its receptor.

The results of this study were published in 2011:

Molina, M. F.; Qu, H. Q.; Rentfro, A. R.; Nair, S.; Lu, Y.; Hanis, C. L.; McCormick, J. B.; Fisher-Hoch, S. P. *Decreased expression of ATP6V1H in type 2 diabetes: a pilot report on the diabetes risk study in Mexican Americans*. Biochem Biophys Res Commun 2011, 412 (4), 728-31.

INTRODUCTION

1. The impact of diabetes

Diabetes, a chronic disease involving the inability of the body to receive sugar properly from the bloodstream, affects an estimated 346 million people worldwide (124). In 2004, diabetes led to the death of approximately 3.4 million people. About 10% of those individuals currently afflicted with diabetes suffer from diabetes type 1, which manifests itself primarily in juveniles and children. The other 90% is comprised of individuals suffering from diabetes type 2, the most common form associated with obesity and physical inactivity (124).

In the United States (US), the Centers for Disease Control (CDC) estimates that 25.8 million adults and children suffer from diabetes, a figure which comprises 8.3% of the American population (16). An even more alarming figure is the number of individuals who have been classified as pre-diabetic: 79 million adults aged 20 years or older. Diabetes has been labeled the seventh leading cause of death in the US (16).

In Texas, 1.7 million persons aged eighteen years and older were diagnosed with diabetes in 2009 according to the Behavioral Risk Factor Surveillance System (BRFSS) survey (113). Specifically among forty-five to sixty-four year olds, it was found that the prevalence of diabetes was significantly higher in Hispanics and African-Americans. The prevalence of diabetes also was found to correlate inversely with education level—groups with a higher level of education, had a lower prevalence of diabetes (113).

These trends have become exaggerated in one particular region of Texas known as the Rio Grande Valley. In 2008, this region was found to have an elevated rate of diabetes, estimated at about three times the national rate (77). Because this region is

comprised principally of Mexican-American individuals, researchers have begun to raise questions as to the genetic basis of diabetes in this population.

2. Diabetes and its complications: an overview

As mentioned previously, diabetes occurs because sugar (i.e. glucose) cannot be properly absorbed from the bloodstream into fat, liver and/or muscle cells (1). A peptide hormone known as insulin mediates this process. Normally, high blood glucose levels trigger the secretion of insulin from the pancreas, which then signals the cells of the body to absorb the glucose for free energy storage. In diabetic individuals, however, one or both of two defects in the process can occur: either insulin is not produced in a sufficient amount, or the cells themselves cannot respond to insulin normally (1).

Individuals with Type 1 diabetes specifically are unable to produce insulin (1). Although the cause of this is unknown, it is thought that an autoimmune response against the pancreatic beta cells plays a role in hindering the proper synthesis of insulin. The most common way of treating individuals with type 1 diabetes is to provide them with insulin, which is to be injected into the body daily (1).

The focus of this work was type 2 diabetes. Type 2 diabetes is by far the most common type, occurring principally in adults (1). Diet is thought to be one of the major factors influencing the late onset of type 2 diabetes and those individuals that develop type 2 diabetes are usually obese. Unlike type 1 diabetes, type 2 diabetes can involve being unable to produce adequate amounts of insulin or being unable to *respond* adequately to insulin. This makes it more difficult to treat. Other risk factors associated with type 2 diabetes, aside from poor diet and excess body weight, appear to be genetics, however, it is still unclear how genetics play into the onset of the disease (1).

There are many serious complications associated with prolonged, elevated blood glucose levels and diabetes (1). Among these are blindness, defective circulation (especially in the lower extremities), elevated blood pressure and cholesterol levels, and kidney and nerve damage (1).

3. Molecular pathobiology of diabetes

The elucidation of the insulin signaling pathway is key in understanding how individuals suffering from diabetes cannot produce or are insensitive to insulin. Insulin signaling begins with elevated plasma glucose levels (2). The glucose in the bloodstream passively enters the pancreatic beta cells through a glucose-specific transporter. In these pancreatic beta cells, it is then metabolized to produce adenosine nucleotide triphosphate (ATP), the energy currency of the cell, which proceeds to bind to a potassium channel on the cell membrane. At low blood glucose levels, this channel is open, however, at high blood glucose levels, ATP is produced and able to bind to the channel, triggering its closure. This closure results in a change in cell membrane potential, which leads to the opening of a voltage-gated calcium channel. The influx of calcium results in a signal cascade that eventually leads to cellular exocytosis of insulin into the bloodstream (2).

The insulin travels through the bloodstream and binds to receptors on a variety of body cells including liver, skeletal and heart muscle cells, in order to trigger the absorption of glucose from the bloodstream. The binding of the insulin to its receptor results in an intracellular signal cascade, which ultimately induces the body cells to respond to elevated blood glucose levels in a variety of ways (i.e. increasing the number of glucose receptors in the membrane, synthesizing glycogen, etc.). The insulin-

receptor complex is internalized so that insulin can be dissociated from the receptor and later degraded. The receptor is then recycled back to the cell membrane.

The mechanism by which insulin is internalized inside of somatic cells is known in detail. As outlined above, the first step in the process is the binding of insulin to its receptor. This binding activates the intracellular domain of the insulin receptor, which is a tyrosine kinase. The kinase phosphorylates downstream targets to initiate intracellular signal transduction. The area of the cell membrane containing the insulin-receptor complexes is then engulfed via endocytosis to form an intracellular vesicle. The vesicle ultimately becomes part of the endosomal apparatus (23). The endocytic compartment of the endosomal apparatus has an acidic pH, which spurs the dissociation of insulin from its receptor. The detachment of insulin from its receptor enables it to be degraded, and the resulting vacant receptor is recycled back to the membrane (23). The acidification of the endosome is thus a very important component in the insulin signaling pathway, and this key process is mediated by an enzyme complex known as the vacuolar ATPase (V-ATPase) (described in more detail, below). This enzyme is a member of a related group of enzymes, the ATPase family.

3.1 The ATPase family

The ATPase family consists of multi-subunit enzymes that hydrolyze ATP, using the energy gathered from the hydrolysis to catalyze a variety of cellular processes. Three ion-pumping classes of transmembrane ATPases have been well studied: P-ATPases, F-ATPases, and V-ATPases (36). Table 1 compares the cellular localization and structural components of the three different classes of transmembrane ATPases.

The P-type ATPases play a vital role both in establishing and maintaining electrochemical gradients across cellular membranes in all eukaryotes and most prokaryotes (13). Before hydrolysis of ATP and ion translocation, an acyl phosphoenzyme intermediate is formed—from which the name “P-ATPase” is derived (36). There are five distinct subfamilies of P-ATPases (P_I – P_V) (5, 4, 112), of which P_{II} and P_{III} are the best studied (5). The Na^+,K^+-ATPases from the P_{IIC} subfamily and the H^+-ATPases from that of P_{III} have been known to energize the plasma membrane for cellular processes such as signaling and secondary active transport (102), whereas the Ca^{2+}-ATPases from that of P_{IIa} restore Ca^{2+} levels in the sarcoplasmic reticulum after muscle contraction (51).

The F-type ATPases are found in inner mitochondrial membranes, eubacterial plasma membranes, and chloroplast thylakoid membranes (22). They are commonly known as “ATP synthases” because they synthesize ATP by utilizing the passive flow of protons down an electrochemical gradient (22). This process, which is accomplished via a rotary mechanism (82), enables them to harness energy for the cell.

The V-ATPases derive their name from the fact that they were originally discovered in plant and fungal vacuoles, however, it is now known that V-ATPases are found in a variety of eukaryotic endomembrane organelles (36). The principle function of V-ATPases is to acidify intracellular compartments by using the energy gathered from ATP hydrolysis to pump protons (107). This gives them an important role in receptor-mediated endocytosis, intracellular trafficking processes, microbial killing (52) and protein degradation (40).

Of particular importance is V-ATPase activity in the endosome. The V-ATPase complex pumps protons into the endosome lumen, creating an acidic environment that not only enables ligand-receptor complexes (brought in from the plasma membrane) to dissociate (39), but also allows for the vesicular trafficking of released ligands from early endosomes to late endosomes (44). Figure 2 summarizes the localizations and functions of V-ATPase.

3.1.1 Comparison of F-ATPase, P-ATPase and V-ATPase

Table 2 compares the three members of the ATPase family. The F-ATPases and V-ATPases are more similar to each other than either is to the P-ATPases. This is because they belong to the rotary ATPase family: membrane complexes that use rotary motor mechanisms to translocate ions across membranes (81). In contrast, the P-type ATPases undergo conformational changes in their transmembrane domains, which facilitate ion translocation (13). Both F-ATPases and V-ATPases are divided into two domains, F_0/V_0 and F_1/V_1, which are involved in ion translocation and ATP hydrolysis, respectively (53). The subunits of F- and V-ATPases shown in the table are aligned based on homology; for example, the β subunit of bovine F-ATPase is homologous to the A subunit of eukaryotic V-ATPase in that both are involved in hydrolyzing ATP. Unlike V-ATPases, F-ATPases have the ability to synthesize ATP: the proton motive force drives the rotation of subunit γ, which provides enough energy for specific sites located on each of the β subunits to catalyze ATP synthesis (22).

3.1.2 V-ATPase structure

The general structure of V-ATPases has yet to be elucidated, however, an approximate structure has been deduced based on both molecular techniques and similarities with other enzymes such as the F-ATPases (107).

V-ATPases contain two functional domains, V_0 and V_1 (40). The V_0 domain is approximately 260-kDa and in yeast, it is composed of five distinct subunits: a, d, c, c', and c,'' which possess a stoichiometry of $a_1d_1c_{4\text{-}5}c'_1c''_1$ (36). Although the exact arrangement of the subunits remains unclear, researchers have concluded that the V_0 domain is an integral domain, which has the potential to conduct protons (107). This conclusion is based on its homology with the F_0 domain of *Escherichia coli*, reassembly studies, and acid treatment (107). Contrary to the V_0 domain, the V_1 domain contains eight subunits (A-H, with stoichiometry $A_3B_3C_1D_1E_3F_1G_3H_1$), which form a peripheral complex believed to be responsible for the hydrolysis of ATP (3, 61).

Of particular interest in the V_1 domain is the latest regulatory subunit of V-ATPase to be identified, subunit H (V1H) (40). In a study performed by Lu and Yang (71) in 2008, protein and mRNA levels of various genes were analyzed in diabetic versus non-diabetic mice using quantitative proteomics and microarray techniques, respectively. These investigators found that both the protein and the mRNA levels of subunit H were lower in diabetic mice, indicating that a down-regulation of V-ATPase subunit H gene expression accompanied the onset of type 2 diabetes in this murine model system (71). Furthermore, in 2011, using pancreatic islets from human patients with type 2 diabetes, Olsson and Yang (84) showed that subunit H gene expression correlated negatively with HbA1c levels and positively with glucose-stimulated insulin

secretion. They did so using microarray gene expression assays. This result suggests that a down-regulation in subunit H gene expression may lead to the impairment of insulin secretion and an increase in HbA1c levels (84).

3.1.3 V-ATPase subunit H – structure and function

The structure of subunit H consists of two domains: the N-domain (amino acids 2-352) and the C-domain (amino acids 353-478) (98). It is highly helical, with seventeen consecutive α-helices in the N-domain, and eight in the C-domain (98). The domains are connected by a small loop containing just four amino acid residues (98). A study which expressed the two domains independently in yeast (in the absence of wild-type subunit H) revealed that while the N-terminal domain was partially able to restore ATP hydrolysis activity in the V-ATPase enzyme, the C-terminal domain neither supported ATP hydrolysis nor proton transport (69). The minimal region of the N-terminal domain needed to restore hydrolysis activity was discovered to be amino acids 180-353 (31). It was concluded that the N-terminal domain was sufficient to catalyze ATP hydrolysis in the V_1 domain, however, the C-terminal domain was still needed to ensure proper communication between the V_1 and V_0 domains (69). It also has been shown that the C-terminal domain of subunit H is necessary in inhibiting ATPase activity of free V_1 domain complexes by interacting with subunit F via a cysteine residue at position 381 (53).

The α-helical motifs in the N-domain of Subunit H show structural similarity to the armadillo or HEAT motifs (an arrangement of three α–helices, each about 42 amino acids in length) found in the importin family of proteins (98). These proteins bind to nuclear localization signals on other proteins via a hydrophobic, shallow groove,

facilitating protein transport from the cytosol into the nucleus (90, 64). The armadillo motifs in subunit H thus present potential binding sites for other proteins.

It is known that the *ATP6V1H* gene encodes for subunit H. The two known isoforms of subunit H that arise from alternative splicing of mRNA have been denominated sub-fifty-eight-kDA dimer (SFD) -α and -β (125). SFD-α contains 18 more amino acids than SFD-β, which correspond to amino acids 178-195 of the yeast subunit H (49, 128). These additional amino acids are found in the N-terminal domain of the subunit (31). Both splice variant mRNAs have been found in brain, kidney, lung and heart tissue, however, the SFD-α isoform appears to be more abundant in all tissues except the brain, where the SFD-β isoform is majority (127). Although only the SFD-α isoform has been extracted from brain chromaffin granules (49, 127), it has been shown that both isoforms can act interchangeably to allow for functional ATPase activity in the V-ATPase of chromaffin granules (127). Thus, there exists no cogent evidence in support of a functional difference between the two isoforms.

It has shown experimentally that subunit H interacts with subunit E (72) and the N-terminal of subunit a (66). Landolt-Marticorena and Williams (66) used binding assays to show that subunit H associates directly with the N-terminal of subunit a both *in vitro* and *in vivo*, suggesting that subunit H may act as a structural link between the V_1 and V_0 domains of V-ATPase (66). Lu and Vegara (72) used dominant-negative mutation studies performed on subunit E and subunit H to reveal that amino acids 1-78 of subunit E are required for sufficient binding to subunit H, which can only reciprocate the interaction as a whole protein. This result suggests that subunit H must fold into a specific conformation in order to interact with subunit E. The interaction between the two

subunits has proven to be necessary for maintaining proper ATPase function, lending support to the theory that both subunits form structural segments of the peripheral stalk of the ATPase complex (72). Figure 1 presents a postulated structure and subunit composition of V-ATPase proposed by the author.

Although the function of subunit H is unknown, it is known that the V-ATPase enzyme cannot function without this subunit. Subunit H is not essential for the assembly of V-ATPase, but it is necessary for the ATPase activity of the enzyme complex (40). Experiments performed by Parra *et al.* (87) in 2000 showed that subunit H can reversibly dissociate from the V-ATPase enzyme complex. When it does so, the free V_1 domains of the complex no longer have ATPase activity (87). This suggests that subunit H may have an important regulatory effect on V-ATPase activity (87). These investigators postulated that this process may prevent the wasteful ATP depletion in the absence of proton translocation (87). If this is true, it would be advantageous for the subunit H to be regulated in some way, whether it be by self-regulation or regulation by some external factor. Sagermann *et al.* (98) have presented evidence that subunit H may self-regulate by either folding back on itself or forming dimers, owing to its structural similarity to the importin family. Alternatively, certain motifs present in the structure of subunit H (discussed below) may serve as binding sites for other proteins outside of the ATPase enzyme complex—thus, providing a way for the enzyme to be externally regulated.

3.2 V-ATPase subunit H and diabetes

While the mechanism by which the down-regulation of subunit H may affect the development of type 2 diabetes remains to be identified, a review of its function in other

cellular processes may provide some clues. Based on a review of the literature, the author would like to offer three hypotheses by which the down-regulation of subunit H of V-ATPase could lead to diabetes: 1) the inhibition of V-ATPase blocks endosomal acidification and prevents the recycling of the insulin receptor back to the cell membrane; 2) a necessary interaction of V-ATPase with ectoapyrase, an enzyme needed for the glycosylation of the insulin receptor, is disrupted, and/or 3) subunit H fails to act as a mediator protein in the internalization of the insulin receptor. The following paragraphs outline these mechanisms and the research supporting them.

Direct evidence for the first hypothesis was provided in 1997, by Benzi *et al.* (6), who demonstrated the importance of the dissociation of the insulin hormone from its receptor. They found that the monocytes from type 2 diabetic patients exhibited reduced binding, internalization and degradation of insulin, along with inhibited recycling of the insulin receptor—all of which were defects associated with ineffective dissociation of the internalized insulin-insulin receptor complex. They compromised endosomal acidification by using an ionophore known as monensin and effectively mimicked the abnormal processing of insulin in patients with non-insulin-dependent diabetes mellitus (type 2 diabetes) (6). When they treated normal cells with monensin they reproduced all of the aforementioned defects except for the decrease in insulin internalization. The results of their study provide strong support to the theory that the dissociation of the insulin-insulin receptor complex in the endosome may be important for further intracellular processing of insulin and its receptor. If this is true, then a down-regulation of subunit H leading to a down-regulation of V-ATPase activity in the endosome could mimic these effects.

Support for the second hypothesis has been provided by multiple investigators. Ectoapyrases play an important role in the glycosylation of proteins and lipids in the golgi apparatus by preventing the accumulation of nucleoside diphosphates, which, if present in sufficient concentrations in the golgi lumen, will inhibit glycosyltransferases (37, 65). Direct binding and coimmunoprecipitation studies have shown that subunit H interacts with an ectoapyrase found in yeast known as Ynd1p (126). Subunit H (while associated with its V-ATPase complex) was shown to repress Ynd1p activity by associating with Ynd1p's cytoplasmic domain (126). This finding is important because it suggests that if subunit H is down-regulated, ectoapyrase activity might become over-reactive and lead to the hyper-glycosylation of various proteins. Several major subunits of the insulin receptor complex consist of glycoproteins (45), which may mean that if glycosyltransferase activity is irregular, insulin receptor activity could also be irregular.

Finally, in 2002, Geyer *et al.* (41) outlined a potential role of subunit H in receptor internalization. They found that the subunit was able to act as an adaptor for an interaction between the Nef protein and a subunit of the adaptor protein complex 2 (AP-2), thus enabling the internalization of CD4 T cell receptors (41). The Nef protein is an important virulence factor, implicated in the progression of HIV in humans. It is believed to enhance viral infectivity by down-regulating CD4 and MHC class I molecules and altering signal transduction pathways in T cells (92). The adaptor protein complex 2 is a heterotetrameric complex that enables endocytotic cage formation by serving as a linker between the cytoplasmic clathrin lattice and proteins embedded in the plasma membrane (88). Geyer *et al.* (41) demonstrated that subunit H interacted with the N-terminal adaptin-binding domain of the medium chain (μ2) of the adaptor protein

complex 2 via four armadillo repeats—common structural motifs composed of alpha helices that form a hairpin structure. An analysis which compared arm repeats in β-catenin, adenomatous polyposis coli (APC) and SRP1 in *Saccharomyces cerevisiae*, suggested that one of the armadillo repeats' main functions could be to mediate specific protein-protein interactions in much the same way as SH2 or ankyrin domains (90). In other words, the armadillo domain in one protein may bind directly to a particular amino acid motif in another protein, which may also contain arm repeats that can bind to a similar motif in a third protein. This model for protein linkage agrees with how the arm repeat structural domain in subunit H was shown to link Nef and AP-2. The fact that the interaction resulted in the internalization of CD4 T cell receptors suggests that the function of subunit H may involve serving as an adaptor for endocytosis and thus, the internalization of the insulin-receptor complexes.

3.3 V-ATPase subunit H and diabetes complications

Diabetic cardiomyopathy

Diabetic cardiomyopathy collectively refers to the diabetes-associated changes in the structure and function of the myocardium that are not thought to be associated with other confounding factors (9). Among the causes of cardiac dysfunction in diabetic cardiomyopathy is cell death, although the mechanism behind this process is not well understood (9).

One possible way in which subunit H could play a role in the cell death of cardiomyocytes was presented by Long *et al.* (70) in 1998. They showed that the inhibition of V-ATPase using bafilomycin A1 induced apoptosis in cardiomyocytes via a pathway involving the p53 protein (70). This suggests that V-ATPase activity prevents

cardiomyocyte apoptosis through a p53 pathway. This finding implies that if *ATP6V1H* is down-regulated, subunit H will not be present to activate the V-ATPase enzyme complex and as a result, V-ATPase may be unable to prevent apoptosis in adult cardiomyocytes.

Diabetic nephropathy

Diabetic nephropathy is another complication of diabetes and is the most common cause of end-stage renal disease in the US (46). It begins with glomerular hyperfiltration and hyperperfusion, and later progresses to mesangial expansion, glomerular hypertrophy and thickening of the glomerular basement membrane (26). One cause of glomerular hyperperfusion and hyperfiltration is the decreased resistance in the arterioles of the glomerulus (26). An increase in nitric oxide, a common vasodilator, is thought to be behind this process (26).

The V-ATPase enzyme complex has been shown to impact nitric oxide production. The inhibition of V-ATPase by bafilomycin A1 and concanamycin A induced nitric oxide (NO) production in the mouse leukemic monocyte cell line RAW 264.7 by increasing iNOS protein expression via the activation of NF-kB and AP-1 (47). This implies that a decrease in V-ATPase activity (induced by the down-regulation of subunit H expression) might also lead to an increase in NO production, and thus, contribute to the hyperperfusion and hyperfiltration found in diabetic nephropathy.

Diabetic neuropathy

Perhaps the most serious of diabetic complications is diabetic neuropathy, which is characterized by damage to peripheral somatic or autonomic nerve fibers (29). The principle causes behind this process originate from hyperglycemia, which disrupts

several pathways in glucose metabolism and ultimately results in an imbalance in the mitochondrial redox state of the nerve cell, leading to the excess formation of reactive oxygen species (ROS) (29). ROS specifically target the post-mitotic glial cells and neurons, resulting in neuronal damage. In humans, this damage has been shown to lead to apoptosis, or programmed cell death (119). Another side effect of hyperglycemia is neuronal ischemia, which results from disruptions in neurovascular flow (29). The down-regulation of V-ATPase activity produced by a shortage of subunit H may contribute to both the formation of ROS and neuronal ischemia, as described below.

There exists an interesting interplay between V-ATPase, ROS and oxidative stress. Hydrogen peroxide, a ROS, has been shown to hinder V-ATPase in brain synaptic vesicles (123). Since the acidification of secretory vesicles is essential for neurotransmitter uptake, this inhibition has the potential to down-regulate neurotransmitter uptake and thus, negatively affect second messenger signaling in the brain (123).

The author would like to propose a mechanism by which V-ATPase could give rise to neuronal ischemia through an enzyme known as cyclooxygenase-2 (COX-2). COX-2 produces inflammatory prostanoids (whose levels are raised in streptozotocion-induced diabetic rats) (50), by breaking down arachidonic acid (26). The inflammation caused by these prostanoids can disrupt circulation by disrupting blood flow. The inhibition of vacuolar ATPase by bafilomycin and concanamycin in a mouse cell line resulted in an increased level of COX-2 and its mRNA (56). The upregulation of COX-2 also has been observed in the peripheral nerves and vascular tissues in experimental diabetes in rats (59) and is believed to contribute to blood flow and nerve conduction

deficits found in diabetic neuropathy (60, 75). One possible way this upregulation could occur is if subunit H is not present to enable functional V-ATPase activity in the brain.

4. Diabetes risk study: the Cameron County Hispanic Cohort (CCHC)

The individuals chosen for this study were part of a 2,500 member cohort established on the US-Mexican border, specifically in Brownsville (Cameron County), Texas. One hundred percent of the individuals in the cohort were Mexican-Americans. Within this group, approximately 49.6% are obese and 30.7% suffer from diabetes. In addition, assessments of the average C-reactive protein levels and alanine transaminase levels indicate that this group also has a particularly high risk of cardiovascular and liver disease, respectively. The elevated risk factors that are found in this cohort make it an ideal focal point for studies analyzing the development of diseases such as diabetes over time. Indeed, over a three-year period, nine individuals in the cohort were documented to progress from pre-diabetes to diabetes, and these individuals were the focus of this research.

The CCHC was established by researchers at The UT School of Public Health, Brownsville Regional Campus (UTSPH-B) to study diabetes among those living in the lower Rio Grande Valley region of Texas. Information about the cohort was generously provided to the author by Dr. Susan P. Fisher-Hoch, Professor of Epidemiology, and Dr. Joseph B. McCormick, Regional Dean and James Steele Professor, UTSPH-B.

The purpose of this research was threefold:

1. To study the demographic and physiological parameters of nine individuals in the CCHC who developed diabetes over the three years of the study period.

2. To investigate whether the gene encoding subunit H of V-ATPase (*ATP6V1H*) was down-regulated in the nine individuals as they progressed from pre-diabetes to type 2 diabetes.
3. To perform an extensive literature review of the *ATP6V1H* gene and its protein product, V-ATPase subunit H, to postulate what role it might play in the development of diabetes and its complications.

METHODS

1. Subjects

The members of the CCHC were recruited door-to-door from households randomly selected in Brownsville area. CCHC participants were seen at the local Clinical Research Unit (CRU), supported by the Center for Clinical and Translational Research Center, and staffed by a team of bilingual nurses and field workers trained in Good Clinical Practices. At the clinic, fasting blood was taken from each cohort member for clinical, metabolic and immunological assays, cytokines and adipokines, DNA, and RNA. Written informed consent was obtained from each participant, and the Committee for the Protection of Human Subjects of The University of Texas Health Science Center at Houston approved this study.

The participants of this particular Diabetes Risk Study totaled 297 and were examined quarterly over three years. Nine of them transitioned from pre-diabetes to overt diabetes during this time, in accordance with standards of the American Diabetes Association. On average, each participant had 4 visits, during which a questionnaire and clinical examination were administered and whole blood was collected (79).

2. Measured Physiological Parameters

After venipuncture, cholesterol and triglycerides were immediately measured using CardioChek bioscanners. The samples were then centrifuged within thirty minutes of collection in a refrigerated centrifuge for twelve minutes at 2000 RPM. After centrifugation, blood glucose values were obtained using plasma in the machine YSI 2300 STAT PLUS. For HDL cholesterol, LDL cholesterol, and HbA1c levels, one milliliter of frozen plasma was sent to the Community Reference Laboratory (Valley

Baptist Medical Center, Harlingen laboratory). It should be noted that hemoglobin A1c (HbA1c) levels were assessed in whole blood collected in 2ml tubes containing ethylenediaminetetraacetic acid (EDTA).

3. Blood RNA purification

After whole blood was collected from the participants in PAXgene Blood RNA tubes, it was centrifuged for ten minutes at 3000-5000xg. The supernatant was then removed with a pipet and the pellet was dissolved in buffer. Proteinase K was then added and the samples were incubated and then recentrifuged. After a series of washing through spin columns and centrifuging at various speeds, a DNase stock solution was added and another series of washing through spin columns and centrifuging ensued. The RNA was then eluted through the spin column into a buffer solution. RNA concentrations were assessed using the NanoDrop ND-1000 UV-Vis Spectrophotometer, and RNA quality was assessed from the electropherogram generated on an Agilent 2100 Bioanalyzer and a RNA integrity number produced by Agilent Expert software (Quebec Genome innovation Center). From 2.5 ml of whole blood, 4-8ug of total RNA was extracted. The protocol for this technique can be found in Appendix A.

4. Microarray analysis and gene expression profiling

Transcriptome profiling of RNA samples from the nine participants was performed with a microarray technique, which utilized the Illumina HumanHT-12 BeadChip (Illumina, San Diego). The samples were shipped to the McGill University and Génome Québec Innovation Centre and the gene expression assays were performed there.

The BeadChip targets over 47,000 probes, thus enabling the assessment of the expression of many thousands of genes at once. The probes on the BeadChip are first hybridized to labeled nucleic acid derived directly from the total RNA and then scanned on the BeadArray reader, iScan system or HiScanSQ system. This enables the results to be read and interpreted. The protocols for this process can be found in Appendix B.

5. Data analysis

Flexarray software was used to analyze the microarray data (8). The data were normalized using the Lumi Bioconductor package implemented in Flexarray (79). A total of 34,694 genes were assayed on the HT-12 BeadChip, and the expression for 22,251 genes was detectable. Twelve thousand four hundred and forty three genes were removed from further analysis because of undetectable expression. The transcriptome profiles of the RNA samples were clustered by each individual participant, instead of by disease status. The transcriptome profile varied between individuals. Because of this phenomenon, a pairwise Z test was selected to compare the differences in gene expression within each individual over time. Statistical significance was corrected for multiple comparisons by the Benjamini and Hochberg False Discovery Rate using QVALUE software (79).

A pairwise T test was used to analyze triglyceride, glucose, cholesterol, high-density lipoprotein (HDL), low-density lipoprotein (LDL), and HbA1c levels in the blood of participants to determine if there was a statistically significant difference between each measure after their first and last visit to the CRU. These tests were conducted at an alpha significance level of 0.05.

RESULTS

1. Participant demographics

As shown in Figure 3, six of the nine participants that developed type 2 diabetes were female, and three were male. Figure 4 shows the distribution of ages of the participants who developed the disease. Five of the participants were between the ages of 60 and 75 (three were between the ages of 60-65, and two were between the ages of 65-75). Three participants were between the ages of 35 and 50, and one participant was 81-years-old. The fact that six of the nine participants were between the ages of 60-81 is not surprising, considering type 2 diabetes usually manifests itself in the later stages of life.

It was also of interest to examine the weight of the participants before and after the onset of diabetes because this disease has been associated with obesity. Measurements were taken on the first and last visits of the participants to the CRU. (The dates of these visits can be seen in Table 3). Figure 5 displays the weights of the participants at their first and last visits. Six of the nine participants (participant 1, 2, 3, 6, 8, 9) experienced weight gain. The other three participants actually underwent weight loss. None of the weight fluctuations varied by more than ten pounds. A paired one-tailed T test was carried out to determine if there was a statistically significant difference in the weights before and after diabetes onset. The test indicated that there was a 5% chance of seeing a difference this great in weights before and after diabetes onset. Since this value was not smaller than an alpha significance level of 0.05, the null hypothesis that the weights in the participants before the development of diabetes were on average less than those after the development of diabetes was rejected. Thus, the

weight differences seen in participants before and after development of diabetes were not statistically significant.

2. Measured physiological parameters

Among the physiological parameters measured were triglyceride, cholesterol, HDL cholesterol and LDL cholesterol, glucose, and HbA1c levels. Figure 6 shows the comparison of triglyceride levels before and after the onset of diabetes for each participant. Although the levels of participant 3, participant 4 and participant 5 didn't vary by over 50mg/dL, the rest of the participants experienced an increase in triglyceride levels of 65mg/dL or more. This increase was statistically significant, with a p-value of 0.01. The differences in cholesterol (Figure 7) between participants before and after diabetes onset did not appear to demonstrate as regular of a pattern. Participant 1, 3, 5 and 6 experienced decreases in cholesterol levels and the highest increase in cholesterol was seen in participant 9 (26mg/dL). These fluctuations did not prove to be statistically significant. Interestingly, the majority of participants (participant 2, 3, 4, 6, 7, 8, 9) experienced increases in HDL cholesterol levels ranging from 3-22mg/dL (Figure 9) and decreases in LDL cholesterol levels (participant 1, 2, 3, 6, 7) ranging from 16 to 38mg/dL (Figure 10). The increases in HDL cholesterol levels were statistically significant with a p-value of 0.027.

The two physiological parameters that were of particular interest to the author were blood glucose and glycosylated hemoglobin HbA1c levels. Glucose levels increased in all nine participants, with increases ranging from 10.5-74.5 mg/dL (Figure 8). The results of the paired T test are shown in Table 4. The calculated t-statistic was 5.47, with a p-level of 0.0003. Based on an alpha statistical significance level of 0.05

and a one-tailed distribution, the null hypothesis that there was no difference between the levels of blood glucose before and after diabetes onset was rejected. Thus, the data showed that the blood glucose levels increased after the development of diabetes in all nine participants by a statistically significant amount.

The data on HbA1c levels were not as conclusive (Figure 11). The percentage of HbA1c actually decreased in six of the participants (participant 2, 3, 4, 6, 8, 9), a result which would not be expected of patients developing diabetes. The results of a two-tailed paired T test are shown in Table 5. The calculated t-statistic was 1.45, giving a p-value of 0.1849. Since this p-value was greater than the alpha significance level of 0.05, the null hypothesis that there was no difference between the HbA1c percentages before and after the development of diabetes could not be rejected. Thus, the data on HbA1c percentages did not indicate that there was a significant difference in the HbA1c levels of the nine participants before and after the development of diabetes.

3. Evidence for down-regulation of the ATP6V1H gene in participants with diabetes

Decreased expression of *ATP6V1H* in peripheral blood was documented with the development of diabetes in each of the nine participants (Figure 12). Among all the genes assayed in this study, the difference of *ATP6V1H* expression between pre-diabetes and overt diabetes was the most significant with an uncorrected p-value of 7.18×10^{-11}, and an FDR corrected q-value of 1.14×10^{-6}. While there was considerable variation observed for each of the individuals with development of diabetes, the expression of *ATP6V1H* decreased in each individual without exception.

DISCUSSION

Because the number of participants that transitioned from pre-diabetes to overt diabetes was very small, it is hard to reach meaningful conclusions about the demographic profile of a typical patient suffering from type 2 diabetes. Six of the nine participants that developed diabetes, however, were over the age of 60—a fact that substantiates that age is an important determining factor in the development of diabetes. Six of the nine participants also experienced weight gain, although the weight gain was not significant.

It was not surprising that a statistically significant increase in blood glucose levels was seen in the nine participants; hyperglycemia is a common condition seen universally in diabetes patients. The statistically significant increase in triglyceride levels might be one side effect of the increase in blood glucose levels; elevated triglyceride levels are often seen in patients with poorly controlled diabetes. It was surprising, however, that the HDL levels showed a statistically significant in seven of the participants and the LDL levels decreased (albeit not statistically significant) in five of the participants. HDL is often associated with decreased risk of cardiovascular disease and usually diabetes is accompanied by an *increased* risk of cardiovascular disease. Similarly, LDL is known as “bad cholesterol” and it wouldn’t follow that the development of diabetes would lead to a decrease in LDL levels. It is likely that these fluctuations were not significant, as the maximum amount the levels varied by was 38mg/dL.

It was also surprising that there was no significant change in HbA1c levels between the participants before and after the onset of diabetes, as one would think that a significant increase in blood glucose levels would also cause an increase in

glycosylated hemoglobin. It is possible that although the blood glucose levels increased significantly, it was not a sufficient enough increase to spur the spontaneous glycosylation of hemoglobin.

There were two novel aspects that differentiated this study from other published works. First, the actual progression of nine individuals from pre-diabetes to diabetes was captured by following them over a period of three years. This is a noteworthy feat, considering the inherent difficulty in predicting when a patient is going to develop a disease. Second, peripheral white blood cell gene expression was innovatively used as a highly accessible source of potential markers for the onset of diabetes.

There is no question that this study has demonstrated a significant down-regulation in the expression of the *ATP6V1H* gene. The aim of researchers, however, is to discover how the down-regulation of this gene is related to the development of type 2 diabetes in Mexican-Americans. In this study, the author proposed three potential explanations: 1) the inhibition of V-ATPase may block endosomal acidification and prevent the recycling of the insulin receptor back to the cell membrane; 2) a necessary interaction of V-ATPase with ectoapyrase, an enzyme needed for the glycosylation of the insulin receptor, might be disrupted and/or 3) subunit H may fail to act as a mediator protein in the internalization of the insulin receptor. Based on an extensive literature review, the author believes the most likely theory is that the V1H subunit is indirectly involved in endosomal acidification, which, in turn, affects the dissociation of the insulin-insulin receptor complex. This is the simplest explanation as blocking V-ATPase activity is known to hinder endosomal acidification, which in turn disrupts the recycling of the insulin receptor. Subunit H is key in enabling this crucial activity of the V-ATPase

enzyme. Support for this hypothesis could be gained by demonstrating that the inhibition of subunit H ultimately results in the disruption of endosomal acidification. Such evidence would provide the link between the observation that the gene for subunit H is down-regulated in diabetic patients and the impairment of the dissociation of the insulin-insulin receptor. In contrast, the author believes that it would require more extensive work to link subunit H to the glycosylation of the insulin receptor and/or to the internalization of the insulin receptor.

As mentioned above, the primary limitation of this study was the small number of participants that acquired diabetes. A greater number of transitioning individuals is needed to reproducibly demonstrate the down-regulation of the *ATP6V1H* gene and to better characterize the individual fluctuations in gene expression that accompanied the onset of diabetes in the nine study participants. A second limitation of this study was that it was not possible to collect more blood samples from each participant in order to get a consistent assessment of gene expression and to minimize individualistic variation. Collecting additional blood samples was difficult to achieve because many participants changed addresses or telephone numbers over the three-year period and were thus difficult to contact.

If the author had the opportunity to continue this work, she would first like to increase the sample size and reexamine the change in *ATP6V1H* gene expression using NanoString technology—a more precise way of assaying gene expression than the microarray technique. Second, she would like to explore the use of mice as model systems since it is likely that they undergo similar changes in gene expression with the onset of diabetes as humans. This would be convenient because mice are more

accessible than humans and have served as useful model systems for other diseases. Finally, the author would like to investigate the expression changes of other candidate genes in diabetes, aside from *ATP6V1H*.

REFERENCES

1. **A.D.A.M.** Diabetes. PubMed Health. U.S. National Library of Medicine, 31 Aug. 2011. [Online] http://www.ncbi.nlm.nih.gov/pubmedhealth/PMH0002194/ Accessed 9 May 2012.

2. **Ashcroft, F. M.; Rorsman, P.**, Diabetes mellitus and the beta cell: the last ten years. Cell 2012, 148 (6), 1160-71.

3. **Arai, H.; Terres, G.; Pink, S.; Forgac, M.**, Topography and subunit stoichiometry of the coated vesicle proton pump. J Biol Chem 1988, 263 (18), 8796-802.

4. **Auland, M. E.; Roufogalis, B. D.; Devaux, P. F.; Zachowski, A.**, Reconstitution of ATP-dependent aminophospholipid translocation in proteoliposomes. Proc Natl Acad Sci U S A 1994, 91 (23), 10938-42.

5. **Axelsen, K. B.; Palmgren, M. G.**, Evolution of substrate specificities in the P-type ATPase superfamily. J Mol Evol 1998, 46 (1), 84-101.

6. **Benzi, L.; Cecchetti, P.; Ciccarone, A. M.; Nardone, A.; Merola, E.; Maggiorelli, R.; Campi, F.; Di Cianni, G.; Navalesi, R.**, Inhibition of endosomal acidification in normal cells mimics the derangements of cellular insulin and insulin-receptor metabolism observed in non-insulin-dependent diabetes mellitus. In Metabolism, United States, 1997; Vol. 46, pp 1259-65.

7. **Bidani, A.; Reisner, B. S.; Haque, A. K.; Wen, J.; Helmer, R. E.; Tuazon, D. M.; Heming, T. A.**, Bactericidal activity of alveolar macrophages is suppressed by V-ATPase inhibition. In Lung, United States, 2000; Vol. 178, pp 91-104.

8. **Blazejczyk, M.; Miron, M.; Nadon, R.,** FlexArray: A Statistical Data Analysis Software for Gene Expression Microarrays, Genome Quebec, Montreal, Canada, 2007.

9. **Boudina, S.; Abel, E. D.**, Diabetic cardiomyopathy, causes and effects. Rev Endocr Metab Disord 2010, 11 (1), 31-9.

10. **Bowman, B. J.; Bowman, E. J.**, Mutations in subunit C of the vacuolar ATPase confer resistance to bafilomycin and identify a conserved antibiotic binding site. In J Biol Chem, United States, 2002; Vol. 277, pp 3965-72.

11. **Bowman, E. J.; Graham, L. A.; Stevens, T. H.; Bowman, B. J.**, The bafilomycin/concanamycin binding site in subunit c of the V-ATPases from Neurospora crassa and Saccharomyces cerevisiae. In J Biol Chem, United States, 2004; Vol. 279, pp 33131-8.

12. **Bowman, E. J.; Siebers, A.; Altendorf, K.**, Bafilomycins: a class of inhibitors of membrane ATPases from microorganisms, animal cells, and plant cells. Proc Natl Acad Sci U S A 1988, 85 (21), 7972-6.

13. **Bublitz, M.; Poulsen, H.; Morth, J. P.; Nissen, P.**, In and out of the cation pumps: P-type ATPase structure revisited. In Curr Opin Struct Biol, 2010 Elsevier Ltd: England, 2010; Vol. 20, pp 431-9.

14. **Carpentier, J. L.**, Insulin receptor internalization: molecular mechanisms and physiopathological implications. Diabetologia 1994, 37 Suppl 2, S117-24.

15. **Carpentier, J. L.; Fehlmann, M.; Van Obberghen, E.; Gorden, P.; Orci, L.**, Insulin receptor internalization and recycling: mechanism and significance. Biochimie 1985, 67 (10-11), 1143-5.

16. **Center for Disease Control and Prevention**. National diabetes fact sheet. 2011. [Online] http://www.cdc.gov/diabetes/pubs/pdf/ndfs_2011.pdf Accessed 9 May 2012.

17. **Choi, K.; Kim, Y. B.**, Molecular mechanism of insulin resistance in obesity and type 2 diabetes. Korean J Intern Med 2010, 25 (2), 119-29.

18. **Clemens, D. L.; Horwitz, M. A.**, Characterization of the Mycobacterium tuberculosis phagosome and evidence that phagosomal maturation is inhibited. J Exp Med 1995, 181 (1), 257-70.

19. **Cusi, K.; Maezono, K.; Osman, A.; Pendergrass, M.; Patti, M. E.; Pratipanawatr, T.; DeFronzo, R. A.; Kahn, C. R.; Mandarino, L. J.**, Insulin resistance differentially affects the PI 3-kinase- and MAP kinase-mediated signaling in human muscle. J Clin Invest 2000, 105 (3), 311-20.

20. **Dechant, R.; Peter, M.**, The N-terminal domain of the V-ATPase subunit 'a' is regulated by pH in vitro and in vivo. In Channels (Austin), United States, 2011; Vol. 5, pp 4-8.

21. **Desjardins, M.; Nzala, N. N.; Corsini, R.; Rondeau, C.**, Maturation of phagosomes is accompanied by changes in their fusion properties and size-selective acquisition of solute materials from endosomes. J Cell Sci 1997, 110 (Pt 18), 2303-14.

22. **Devenish, R. J.; Prescott, M.; Rodgers, A. J.**, The structure and function of mitochondrial F1F0-ATP synthases. In Int Rev Cell Mol Biol, Netherlands, 2008; Vol. 267, pp 1-58.

23. **Di Guglielmo, G. M.; Drake, P. G.; Baass, P. C.; Authier, F.; Posner, B. I.; Bergeron, J. J.**, Insulin receptor internalization and signalling. Mol Cell Biochem 1998, 182 (1-2), 59-63.

24. Diagnosis and classification of diabetes mellitus. In Diabetes Care, United States, 2009; Vol. 32 Suppl 1, pp S62-7.

25. **Dooley, K. E.; Chaisson, R. E.**, Tuberculosis and diabetes mellitus: convergence of two epidemics. In Lancet Infect Dis, United States, 2009; Vol. 9, pp 737-46.

26. **Dronavalli, S.; Duka, I.; Bakris, G. L.**, The pathogenesis of diabetic nephropathy. In Nat Clin Pract Endocrinol Metab, England, 2008; Vol. 4, pp 444-52.

27. **Drose, S.; Bindseil, K. U.; Bowman, E. J.; Siebers, A.; Zeeck, A.; Altendorf, K.**, Inhibitory effect of modified bafilomycins and concanamycins on P- and V-type adenosinetriphosphatases. Biochemistry 1993, 32 (15), 3902-6.

28. **Duckworth, W. C.**, Insulin degradation: mechanisms, products, and significance. Endocr Rev 1988, 9 (3), 319-45.

29. **Edwards, J. L.; Vincent, A. M.; Cheng, H. T.; Feldman, E. L.**, Diabetic neuropathy: mechanisms to management. In Pharmacol Ther, England, 2008; Vol. 120, pp 1-34.

30. **Enjyoji, K.; Kotani, K.; Thukral, C.; Blumel, B.; Sun, X.; Wu, Y.; Imai, M.; Friedman, D.; Csizmadia, E.; Bleibel, W.; Kahn, B. B.; Robson, S. C.**, Deletion of cd39/entpd1 results in hepatic insulin resistance. In Diabetes, United States, 2008; Vol. 57, pp 2311-20.

31. **Flannery, A. R.; Stevens, T. H.**, Functional characterization of the N-terminal domain of subunit H (Vma13p) of the yeast vacuolar ATPase. In J Biol Chem, United States, 2008; Vol. 283, pp 29099-108.

32. **Forgac, M.**, Vacuolar ATPases: rotary proton pumps in physiology and pathophysiology. In Nat Rev Mol Cell Biol, England, 2007; Vol. 8, pp 917-29.

33. **Fratti, R. A.; Backer, J. M.; Gruenberg, J.; Corvera, S.; Deretic, V.**, Role of phosphatidylinositol 3-kinase and Rab5 effectors in phagosomal biogenesis and mycobacterial phagosome maturation arrest. In J Cell Biol, United States, 2001; Vol. 154, pp 631-44.

34. **Freeman, T. C.; Raza, S.; Theocharidis, A.; Ghazal, P.**, The mEPN scheme: an intuitive and flexible graphical system for rendering biological pathways. In BMC Syst Biol, England, 2010; Vol. 4, p 65.

35. **Frustaci, A.; Kajstura, J.; Chimenti, C.; Jakoniuk, I.; Leri, A.; Maseri, A.; Nadal-Ginard, B.; Anversa, P.**, Myocardial cell death in human diabetes. Circ Res 2000, 87 (12), 1123-32.

36. **Futai, M.; Wada, Y.; Kaplan, J. H.**, Handbook of ATPases: Biochemistry, Cell Biology, Pathophysiology. Wiley-VCH: Weinheim, 2004.

37. **Gao, X. D.; Kaigorodov, V.; Jigami, Y.**, YND1, a homologue of GDA1, encodes membrane-bound apyrase required for Golgi N- and O-glycosylation in Saccharomyces cerevisiae. J Biol Chem 1999, 274 (30), 21450-6.

38. **Germanov, E.; Berman, J. N.; Guernsey, D. L.**, Current and future approaches for the therapeutic targeting of metastasis (review). Int J Mol Med 2006, 18 (6), 1025-36.

39. **Geuze, H. J.; Slot, J. W.; Strous, G. J.; Lodish, H. F.; Schwartz, A. L.**, Intracellular site of asialoglycoprotein receptor-ligand uncoupling: double-label immunoelectron microscopy during receptor-mediated endocytosis. In Cell, United States, 1983; Vol. 32, pp 277-87.

40. **Geyer, M.; Fackler, O. T.; Peterlin, B. M.**, Subunit H of the V-ATPase involved in endocytosis shows homology to beta-adaptins. Mol Biol Cell 2002, 13 (6), 2045-56.

41. **Geyer, M.; Yu, H.; Mandic, R.; Linnemann, T.; Zheng, Y. H.; Fackler, O. T.; Peterlin, B. M.**, Subunit H of the V-ATPase binds to the medium chain of adaptor protein complex 2 and connects Nef to the endocytic machinery. In J Biol Chem, United States, 2002; Vol. 277, pp 28521-9.

42. **Ghigo, E.; Capo, C.; Aurouze, M.; Tung, C. H.; Gorvel, J. P.; Raoult, D.; Mege, J. L.**, Survival of Tropheryma whipplei, the agent of Whipple's disease, requires phagosome acidification. Infect Immun 2002, 70 (3), 1501-6.

43. **Ghosh, P.; Dahms, N. M.; Kornfeld, S.**, Mannose 6-phosphate receptors: new twists in the tale. In Nat Rev Mol Cell Biol, England, 2003; Vol. 4, pp 202-12.

44. **Gu, F.; Gruenberg, J.**, ARF1 regulates pH-dependent COP functions in the early endocytic pathway. J Biol Chem 2000, 275 (11), 8154-60.

45. **Hedo, J. A.; Kasuga, M.; Van Obberghen, E.; Roth, J.; Kahn, C. R.**, Direct demonstration of glycosylation of insulin receptor subunits by biosynthetic and external labeling: evidence for heterogeneity. Proc Natl Acad Sci U S A 1981, 78 (8), 4791-5.

46. **Held, P. J.; Port, F. K.; Webb, R. L.; Wolfe, R. A.; Garcia, J. R.; Blagg, C. R.; Agodoa, L. Y.**, The United States Renal Data System's 1991 annual data report: an introduction. Am J Kidney Dis 1991, 18 (5 Suppl 2), 1-16.

47. **Hong, J.; Nakano, Y.; Yokomakura, A.; Ishihara, K.; Kim, S.; Kang, Y. S.; Ohuchi, K.**, Nitric oxide production by the vacuolar-type (H+)-ATPase inhibitors bafilomycin A1 and concanamycin A and its possible role in apoptosis in RAW 264.7 cells. In J Pharmacol Exp Ther, United States, 2006; Vol. 319, pp 672-81.

48. **Hu, Y.; Nyman, J.; Muhonen, P.; Vaananen, H. K.; Laitala-Leinonen, T.**, Inhibition of the osteoclast V-ATPase by small interfering RNAs. In FEBS Lett, Netherlands, 2005; Vol. 579, pp 4937-42.

49. **Hui, D.; Deppe, A.; Wen, G.; Leeb, T.; Masabanda, J.; Robic, A.; Baumgartner, B. G.; Fries, R.; Brenig, B.**, Molecular cloning and chromosomal assignment of the porcine 54 and 56 kDa vacuolar H(+)-ATPase subunit gene (V-ATPase). Mamm Genome 1999, 10 (3), 266-70.

50. **Imig, J. D.**, Eicosanoids and renal vascular function in diseases. In Clin Sci (Lond), England, 2006; Vol. 111, pp 21-34.

51. **Inesi, G.; Prasad, A. M.; Pilankatta, R.**, The Ca2+ ATPase of cardiac sarcoplasmic reticulum: Physiological role and relevance to diseases. In Biochem Biophys Res Commun, United States, 2008; Vol. 369, pp 182-7.

52. **Ip, W. K.; Sokolovska, A.; Charriere, G. M.; Boyer, L.; Dejardin, S.; Cappillino, M. P.; Yantosca, L. M.; Takahashi, K.; Moore, K. J.; Lacy-Hulbert, A.; Stuart, L. M.**, Phagocytosis and phagosome acidification are required for pathogen processing and MyD88-dependent responses to Staphylococcus aureus. In J Immunol, United States, 2010; Vol. 184, pp 7071-81.

53. **Jefferies, K. C.; Cipriano, D. J.; Forgac, M.**, Function, structure and regulation of the vacuolar (H+)-ATPases. In Arch Biochem Biophys, United States, 2008; Vol. 476, pp 33-42.

54. **Jeon, C. Y.; Murray, M. B.**, Diabetes mellitus increases the risk of active tuberculosis: a systematic review of 13 observational studies. In PLoS Med, United States, 2008; Vol. 5, p e152.

55. **Kakinuma, Y.; Ohsumi, Y.; Anraku, Y.**, Properties of H+-translocating adenosine triphosphatase in vacuolar membranes of SAccharomyces cerevisiae. J Biol Chem 1981, 256 (21), 10859-63.

56. **Kamachi, F.; Yanai, M.; Ban, H. S.; Ishihara, K.; Hong, J.; Ohuchi, K.; Hirasawa, N.**, Involvement of Na+/H+ exchangers in induction of

cyclooxygenase-2 by vacuolar-type (H+)-ATPase inhibitors in RAW 264 cells. In FEBS Lett, Netherlands, 2007; Vol. 581, pp 4633-8.

57. **Karet, F. E.; Finberg, K. E.; Nelson, R. D.; Nayir, A.; Mocan, H.; Sanjad, S. A.; Rodriguez-Soriano, J.; Santos, F.; Cremers, C. W.; Di Pietro, A.; Hoffbrand, B. I.; Winiarski, J.; Bakkaloglu, A.; Ozen, S.; Dusunsel, R.; Goodyer, P.; Hulton, S. A.; Wu, D. K.; Skvorak, A. B.; Morton, C. C.; Cunningham, M. J.; Jha, V.; Lifton, R. P.**, Mutations in the gene encoding B1 subunit of H+-ATPase cause renal tubular acidosis with sensorineural deafness. Nat Genet 1999, 21 (1), 84-90.

58. **Kawasaki-Nishi, S.; Bowers, K.; Nishi, T.; Forgac, M.; Stevens, T. H.**, The amino-terminal domain of the vacuolar proton-translocating ATPase a subunit controls targeting and in vivo dissociation, and the carboxyl-terminal domain affects coupling of proton transport and ATP hydrolysis. In J Biol Chem, United States, 2001; Vol. 276, pp 47411-20.

59. **Kellogg, A. P.; Pop-Busui, R.**, Peripheral nerve dysfunction in experimental diabetes is mediated by cyclooxygenase-2 and oxidative stress. Antioxid Redox Signal 2005, 7 (11-12), 1521-9.

60. **Kellogg, A. P.; Wiggin, T. D.; Larkin, D. D.; Hayes, J. M.; Stevens, M. J.; Pop-Busui, R.**, Protective effects of cyclooxygenase-2 gene inactivation against peripheral nerve dysfunction and intraepidermal nerve fiber loss in experimental diabetes. In Diabetes, United States, 2007; Vol. 56, pp 2997-3005.

61. **Kitagawa, N.; Mazon, H.; Heck, A. J.; Wilkens, S.**, Stoichiometry of the peripheral stalk subunits E and G of yeast V1-ATPase determined by mass spectrometry. In J Biol Chem, United States, 2008; Vol. 283, pp 3329-37.

62. **Klionsky, D. J.; Nelson, H.; Nelson, N.**, Compartment acidification is required for efficient sorting of proteins to the vacuole in Saccharomyces cerevisiae. J Biol Chem 1992, 267 (5), 3416-22.

63. **Knutson, V. P.**, Cellular trafficking and processing of the insulin receptor. FASEB J 1991, 5 (8), 2130-8.

64. **Kobe, B.**, Autoinhibition by an internal nuclear localization signal revealed by the crystal structure of mammalian importin alpha. Nat Struct Biol 1999, 6 (4), 388-97.

65. **Kuhn, N. J.; White, A.**, The role of nucleoside diphosphatase in a uridine nucleotide cycle associated with lactose synthesis in rat mammary-gland Golgi apparatus. Biochem J 1977, 168 (3), 423-33.

66. **Landolt-Marticorena, C.; Williams, K. M.; Correa, J.; Chen, W.; Manolson, M. F.**, Evidence that the NH2 terminus of vph1p, an integral subunit of the V0 sector of the yeast V-ATPase, interacts directly with the Vma1p and Vma13p subunits of the V1 sector. In J Biol Chem, United States, 2000; Vol. 275, pp 15449-57.

67. **Lee, B. Y.; Jethwaney, D.; Schilling, B.; Clemens, D. L.; Gibson, B. W.; Horwitz, M. A.**, The Mycobacterium bovis bacille Calmette-Guerin phagosome proteome. In Mol Cell Proteomics, United States, 2010; Vol. 9, pp 32-53.

68. **Levy, D.; Zochodne, D. W.**, NO pain: potential roles of nitric oxide in neuropathic pain. In Pain Pract, United States, 2004; Vol. 4, pp 11-8.

69. **Liu, M.; Tarsio, M.; Charsky, C. M.; Kane, P. M.**, Structural and functional separation of the N- and C-terminal domains of the yeast V-ATPase subunit H. In J Biol Chem, United States, 2005; Vol. 280, pp 36978-85.

70. **Long, X.; Crow, M. T.; Sollott, S. J.; O'Neill, L.; Menees, D. S.; de Lourdes Hipolito, M.; Boluyt, M. O.; Asai, T.; Lakatta, E. G.**, Enhanced expression of p53 and apoptosis induced by blockade of the vacuolar proton ATPase in cardiomyocytes. J Clin Invest 1998, 101 (6), 1453-61.

71. **Lu, H.; Yang, Y.; Allister, E. M.; Wijesekara, N.; Wheeler, M. B.**, The identification of potential factors associated with the development of type 2 diabetes: a quantitative proteomics approach. In Mol Cell Proteomics, United States, 2008; Vol. 7, pp 1434-51.

72. **Lu, M.; Vergara, S.; Zhang, L.; Holliday, L. S.; Aris, J.; Gluck, S. L.**, The amino-terminal domain of the E subunit of vacuolar H(+)-ATPase (V-ATPase) interacts with the H subunit and is required for V-ATPase function. In J Biol Chem, United States, 2002; Vol. 277, pp 38409-15.

73. **Lu, X.; Yu, H.; Liu, S. H.; Brodsky, F. M.; Peterlin, B. M.**, Interactions between HIV1 Nef and vacuolar ATPase facilitate the internalization of CD4. In Immunity, United States, 1998; Vol. 8, pp 647-56.

74. **Malikova, M.; Shi, J.; Kandror, K. V.**, V-type ATPase is involved in biogenesis of GLUT4 vesicles. In Am J Physiol Endocrinol Metab, United States, 2004; Vol. 287, pp E547-52.

75. **Matsunaga, A.; Kawamoto, M.; Shiraishi, S.; Yasuda, T.; Kajiyama, S.; Kurita, S.; Yuge, O.**, Intrathecally administered COX-2 but not COX-1 or COX-3 inhibitors attenuate streptozotocin-induced mechanical hyperalgesia in rats. In Eur J Pharmacol, Netherlands, 2007; Vol. 554, pp 12-7.

76. **McDonald, D. S.; Cheng, C.; Martinez, J. A.; Zochodne, D. W.**, Regenerative arrest of inflamed peripheral nerves: role of nitric oxide. In Neuroreport, England, 2007; Vol. 18, pp 1635-40.

77. Medical News Today. Texas' Rio Grande Valley region has high diabetes rate; large Hispanic population considered contributing factor. 2008. [Online] http://www.medicalnewstoday.com/releases/119040.php Accessed 9 May 2012.

78. **Milgrom, E.; Diab, H.; Middleton, F.; Kane, P. M.**, Loss of vacuolar proton-translocating ATPase activity in yeast results in chronic oxidative stress. In J Biol Chem, United States, 2007; Vol. 282, pp 7125-36.

79. **Molina, M. F.; Qu, H. Q.; Rentfro, A. R.; Nair, S.; Lu, Y.; Hanis, C. L.; McCormick, J. B.; Fisher-Hoch, S. P.**, Decreased expression of ATP6V1H in type 2 diabetes: a pilot report on the diabetes risk study in Mexican Americans. Biochem Biophys Res Commun 2011, 412 (4), 728-31.

80. **Moriyama, Y.; Maeda, M.; Futai, M.**, The role of V-ATPase in neuronal and endocrine systems. J Exp Biol 1992, 172, 171-8.

81. **Muench, S. P.; Trinick, J.; Harrison, M. A.**, Structural divergence of the rotary ATPases. In Q Rev Biophys, 2011; pp 1-46.

82. **Noji, H.; Yasuda, R.; Yoshida, M.; Kinosita, K., Jr.**, Direct observation of the rotation of F1-ATPase. Nature 1997, 386 (6622), 299-302.

83. **Obrosova, I. G.; Drel, V. R.; Oltman, C. L.; Mashtalir, N.; Tibrewala, J.; Groves, J. T.; Yorek, M. A.**, Role of nitrosative stress in early neuropathy and vascular dysfunction in streptozotocin-diabetic rats. In Am J Physiol Endocrinol Metab, United States, 2007; Vol. 293, pp E1645-55.

84. **Olsson, A. H.; Yang, B. T.; Hall, E.; Taneera, J.; Salehi, A.; Dekker Nitert, M.; Ling, C.**, Decreased expression of genes involved in oxidative phosphorylation in human pancreatic islets from patients with type 2 diabetes. In Eur J Endocrinol, 2011.

85. **Owegi, M. A.; Pappas, D. L.; Finch, M. W., Jr.; Bilbo, S. A.; Resendiz, C. A.; Jacquemin, L. J.; Warrier, A.; Trombley, J. D.; McCulloch, K. M.; Margalef, K. L.; Mertz, M. J.; Storms, J. M.; Damin, C. A.; Parra, K. J.**, Identification of a domain in the V0 subunit d that is critical for coupling of the yeast vacuolar proton-translocating ATPase. In J Biol Chem, United States, 2006; Vol. 281, pp 30001-14.

86. **Parikh, H.; Nilsson, E.; Ling, C.; Poulsen, P.; Almgren, P.; Nittby, H.; Eriksson, K. F.; Vaag, A.; Groop, L. C.**, Molecular correlates for maximal

oxygen uptake and type 1 fibers. In Am J Physiol Endocrinol Metab, United States, 2008; Vol. 294, pp E1152-9.

87. **Parra, K. J.; Keenan, K. L.; Kane, P. M.**, The H subunit (Vma13p) of the yeast V-ATPase inhibits the ATPase activity of cytosolic V1 complexes. In J Biol Chem, United States, 2000; Vol. 275, pp 21761-7.

88. **Pearse, B. M.; Smith, C. J.; Owen, D. J.**, Clathrin coat construction in endocytosis. In Curr Opin Struct Biol, England, 2000; Vol. 10, pp 220-8.

89. **Pedersen, P. L.; Amzel, L. M.**, F-type ATPases. Introduction. J Bioenerg Biomembr 1992, 24 (5), 427-8.

90. **Peifer, M.; Berg, S.; Reynolds, A. B.**, A repeating amino acid motif shared by proteins with diverse cellular roles. In Cell, United States, 1994; Vol. 76, pp 789-91.

91. **Pietrement, C.; Sun-Wada, G. H.; Silva, N. D.; McKee, M.; Marshansky, V.; Brown, D.; Futai, M.; Breton, S.**, Distinct expression patterns of different subunit isoforms of the V-ATPase in the rat epididymis. In Biol Reprod, United States, 2006; Vol. 74, pp 185-94.

92. **Piguet, V.; Trono, D.**, The Nef protein of primate lentiviruses. In Rev Med Virol, England, 1999; Vol. 9, pp 111-20.

93. **Pitt, A.; Mayorga, L. S.; Stahl, P. D.; Schwartz, A. L.**, Alterations in the protein composition of maturing phagosomes. J Clin Invest 1992, 90 (5), 1978-83.

94. **Powell, B.; Graham, L. A.; Stevens, T. H.**, Molecular characterization of the yeast vacuolar H+-ATPase proton pore. In J Biol Chem, United States, 2000; Vol. 275, pp 23654-60.

95. **Rapoport, I.; Chen, Y. C.; Cupers, P.; Shoelson, S. E.; Kirchhausen, T.**, Dileucine-based sorting signals bind to the beta chain of AP-1 at a site distinct and regulated differently from the tyrosine-based motif-binding site. EMBO J 1998, 17 (8), 2148-55.

96. **Rojas, J. D.; Sennoune, S. R.; Maiti, D.; Bakunts, K.; Reuveni, M.; Sanka, S. C.; Martinez, G. M.; Seftor, E. A.; Meininger, C. J.; Wu, G.; Wesson, D. E.; Hendrix, M. J.; Martinez-Zaguilan, R.**, Vacuolar-type H+-ATPases at the plasma membrane regulate pH and cell migration in microvascular endothelial cells. In Am J Physiol Heart Circ Physiol, United States, 2006; Vol. 291, pp H1147-57.

97. **Rojas, J. D.; Sennoune, S. R.; Martinez, G. M.; Bakunts, K.; Meininger, C. J.; Wu, G.; Wesson, D. E.; Seftor, E. A.; Hendrix, M. J.; Martinez-Zaguilan, R.**,

Plasmalemmal vacuolar H+-ATPase is decreased in microvascular endothelial cells from a diabetic model. J Cell Physiol 2004, 201 (2), 190-200.

98. **Sagermann, M.; Stevens, T. H.; Matthews, B. W.**, Crystal structure of the regulatory subunit H of the V-type ATPase of Saccharomyces cerevisiae. In Proc Natl Acad Sci U S A, United States, 2001; Vol. 98, pp 7134-9.

99. **Saroussi, S.; Nelson, N.**, Vacuolar H(+)-ATPase-an enzyme for all seasons. Pflugers Arch 2009, 457 (3), 581-7.

100. **Sennoune, S. R.; Martinez-Zaguilan, R.**, Plasmalemmal vacuolar H+-ATPases in angiogenesis, diabetes and cancer. J Bioenerg Biomembr 2007, 39 (5-6), 427-33.

101. **Sharma, S.; Adrogue, J. V.; Golfman, L.; Uray, I.; Lemm, J.; Youker, K.; Noon, G. P.; Frazier, O. H.; Taegtmeyer, H.**, Intramyocardial lipid accumulation in the failing human heart resembles the lipotoxic rat heart. In FASEB J, United States, 2004; Vol. 18, pp 1692-700.

102. **Skulachev, V. P.**, Bioenergetics: the evolution of molecular mechanisms and the development of bioenergetic concepts. Antonie Van Leeuwenhoek 1994, 65 (4), 271-84.

103. **Smardon, A. M.; Kane, P. M.**, RAVE is essential for the efficient assembly of the C subunit with the vacuolar H(+)-ATPase. In J Biol Chem, United States, 2007; Vol. 282, pp 26185-94.

104. **Smardon, A. M.; Tarsio, M.; Kane, P. M.**, The RAVE complex is essential for stable assembly of the yeast V-ATPase. In J Biol Chem, United States, 2002; Vol. 277, pp 13831-9.

105. **Smith, A. N.; Jouret, F.; Bord, S.; Borthwick, K. J.; Al-Lamki, R. S.; Wagner, C. A.; Ireland, D. C.; Cormier-Daire, V.; Frattini, A.; Villa, A.; Kornak, U.; Devuyst, O.; Karet, F. E.**, Vacuolar H+-ATPase d2 subunit: molecular characterization, developmental regulation, and localization to specialized proton pumps in kidney and bone. In J Am Soc Nephrol, United States, 2005; Vol. 16, pp 1245-56.

106. **Stelzl, U.; Worm, U.; Lalowski, M.; Haenig, C.; Brembeck, F. H.; Goehler, H.; Stroedicke, M.; Zenkner, M.; Schoenherr, A.; Koeppen, S.; Timm, J.; Mintzlaff, S.; Abraham, C.; Bock, N.; Kietzmann, S.; Goedde, A.; Toksoz, E.; Droege, A.; Krobitsch, S.; Korn, B.; Birchmeier, W.; Lehrach, H.; Wanker, E. E.**, A human protein-protein interaction network: a resource for annotating the proteome. In Cell, United States, 2005; Vol. 122, pp 957-68.

107. **Stevens, T. H.; Forgac, M.**, Structure, function and regulation of the vacuolar (H+)-ATPase. Annu Rev Cell Dev Biol 1997, 13, 779-808.

108. **Sturgill-Koszycki, S.; Schlesinger, P. H.; Chakraborty, P.; Haddix, P. L.; Collins, H. L.; Fok, A. K.; Allen, R. D.; Gluck, S. L.; Heuser, J.; Russell, D. G.**, Lack of acidification in Mycobacterium phagosomes produced by exclusion of the vesicular proton-ATPase. Science 1994, 263 (5147), 678-81.

109. **Sun, G.; Kashyap, S. R.**, Cancer risk in type 2 diabetes mellitus: metabolic links and therapeutic considerations. J Nutr Metab 2011, 2011, 708183.

110. **Sun-Wada, G. H.; Toyomura, T.; Murata, Y.; Yamamoto, A.; Futai, M.; Wada, Y.**, The a3 isoform of V-ATPase regulates insulin secretion from pancreatic beta-cells. In J Cell Sci, England, 2006; Vol. 119, pp 4531-40.

111. **Tang, X.; Halleck, M. S.; Schlegel, R. A.; Williamson, P.**, A subfamily of P-type ATPases with aminophospholipid transporting activity. Science 1996, 272 (5267), 1495-7.

112. **Teitelbaum, S. L.**, Bone resorption by osteoclasts. In Science, United States, 2000; Vol. 289, pp 1504-8.

113. **Texas Department of State Health Services**. Diabetes data: surveillance and evaluation. 2012. [Online] http://www.dshs.state.tx.us/diabetes/tdcdata.shtm Accessed 9 May 2012.

114. **Tiranti, V.; Viscomi, C.; Hildebrandt, T.; Di Meo, I.; Mineri, R.; Tiveron, C.; Levitt, M. D.; Prelle, A.; Fagiolari, G.; Rimoldi, M.; Zeviani, M.**, Loss of ETHE1, a mitochondrial dioxygenase, causes fatal sulfide toxicity in ethylmalonic encephalopathy. In Nat Med, United States, 2009; Vol. 15, pp 200-5.

115. **Toei, M.; Saum, R.; Forgac, M.**, Regulation and isoform function of the V-ATPases. Biochemistry 2010, 49 (23), 4715-23.

116. **Toyomura, T.; Murata, Y.; Yamamoto, A.; Oka, T.; Sun-Wada, G. H.; Wada, Y.; Futai, M.**, From lysosomes to the plasma membrane: localization of vacuolar-type H+ -ATPase with the a3 isoform during osteoclast differentiation. In J Biol Chem, United States, 2003; Vol. 278, pp 22023-30.

117. **Trombetta, E. S.; Ebersold, M.; Garrett, W.; Pypaert, M.; Mellman, I.**, Activation of lysosomal function during dendritic cell maturation. In Science, United States, 2003; Vol. 299, pp 1400-3.

118. **Tycko, B.; Maxfield, F. R.**, Rapid acidification of endocytic vesicles containing alpha 2-macroglobulin. In Cell, United States, 1982; Vol. 28, pp 643-51.

119. **Uttara, B.; Singh, A. V.; Zamboni, P.; Mahajan, R. T.**, Oxidative stress and neurodegenerative diseases: a review of upstream and\ downstream antioxidant therapeutic options. In Curr Neuropharmacol, 2009; Vol. 7, pp 65-74.

120. **Vieira, O. V.; Botelho, R. J.; Grinstein, S.**, Phagosome maturation: aging gracefully. In Biochem J, England, 2002; Vol. 366, pp 689-704.

121. **Vigneri, P.; Frasca, F.; Sciacca, L.; Pandini, G.; Vigneri, R.**, Diabetes and cancer. In Endocr Relat Cancer, England, 2009; Vol. 16, pp 1103-23.

122. **Wang, Y.; Cipriano, D. J.; Forgac, M.**, Arrangement of subunits in the proteolipid ring of the V-ATPase. In J Biol Chem, United States, 2007; Vol. 282, pp 34058-65.

123. **Wang, Y.; Floor, E.**, Hydrogen peroxide inhibits the vacuolar H+-ATPase in brain synaptic vesicles at micromolar concentrations. J Neurochem 1998, 70 (2), 646-52.

124. **World Health Organization**. Diabetes fact sheet. 2011. [Online] http://www.who.int/mediacentre/factsheets/fs312/en/ Accessed 9 May 2012.

125. **Xie, X. S.; Crider, B. P.; Ma, Y. M.; Stone, D. K.**, Role of a 50-57-kDa polypeptide heterodimer in the function of the clathrin-coated vesicle proton pump. J Biol Chem 1994, 269 (41), 25809-15.

126. **Zhong, X.; Malhotra, R.; Guidotti, G.**, Regulation of yeast ectoapyrase ynd1p activity by activator subunit Vma13p of vacuolar H+-ATPase. In J Biol Chem, United States, 2000; Vol. 275, pp 35592-9.

127. **Zhou, Z.; Peng, S. B.; Crider, B. P.; Andersen, P.; Xie, X. S.; Stone, D. K.**, Recombinant SFD isoforms activate vacuolar proton pumps. J Biol Chem 1999, 274 (22), 15913-9.

128. **Zhou, Z.; Peng, S. B.; Crider, B. P.; Slaughter, C.; Xie, X. S.; Stone, D. K.**, Molecular characterization of the 50- and 57-kDa subunits of the bovine vacuolar proton pump. J Biol Chem 1998, 273 (10), 5878-84.

Tables and Figures

Table 1. Summary of cellular localization of P-ATPases, F-ATPases and V- ATPases

ATPase Type	Cellular Localization (Organelle)	ATPase Function
P	Plasma membrane; sarcoplasmic reticulum[1]	Signaling, secondary transport; restoration of Ca^{2+} levels[2]
F	Mitochondrial inner membrane, eubacterial plasma membrane, chloroplast thylakoid membrane[3]	ATP synthesis via electrochemical gradient[3]
V	lysosomes, central vacuoles, secretory vesicles, endosomes, plasma membrane[4]	Functions vary

[1] (Skulachev, 1994)
[2] (Inesi and Prasad, 2008)
[3] (Devenish and Prescott, 2008)
[4] (Forgac, 2007)

Table 2. Structural comparison of P-ATPase, F-ATPase and V-ATPase

P-ATPase[1]			F-ATPase (bovine mitochondria)[2]			V-ATPase (eukaryotic)[3]		
Domain	**Subunit**	**Function**	**Domain**	**Subunit**	**Function**	**Domain**	**Subunit**	**Function**
N (nucleotide binding)	α	ATP hydrolyzing activity	F_1	β (3)[4]	formation and hydrolysis of ATP	V_1	A (3)	hydrolysis of ATP
P (phosphorylation)	α		F_1	α (3)		V_1	B (3)	
A (actuator)	α		-	-		V_1	C	
transmembrane	α	ion transport	F_1	γ		V_1	D	
-	-	-	F_1	OSCP		V_1	E (3)	
-	-	-	-	-		V_1	F	
-	-	-	F_1	δ		-	-	
-	-	-	F_1	ε		-	-	
-	-	-	F_0	*b*	ion translocation	V_1	G (3)	
-	-	-	-	-		V_1	H	
-	-	-	F_0	*a*		V_0	*a*	proton translocation
-	-	-	F_0	*c*		V_0	*c* (10)[5]	
-	-	-	-	-		V_0	*d*	
-	-	-	F_1	*d*	formation and hydrolysis of ATP	-	-	
-	-	-	-	-		V_0	*e*	
-	-	-	F_1	F_6		-	-	-
-	-	-	F_0	A6L	ion translocation	-	-	-
-	-	-	F_0	*e, f, g, i/j*		-	-	-

[1] Adapted from Bublitz and Poulsen, 2010.
[2] Adapted from Muench and Trinick, 2011.
[3] Adapted from Muench and Trinick, 2011
[4] Numbers in parentheses indicate the number of subunits in the enzyme
[5] Stoichiometry and subunit isoforms vary in different species (Powell and Graham, 2000, Wang and Cipriano, 2007).

Table 3. Date of participants' first/last visit

Participant	1	2	3	4	5	6	7	8	9
First Visit Date:	May 1, 2004	July 23, 2004	June 8, 2005	October 13, 2005	November 28, 2005	April 12, 2006	April 13, 2006	June 20, 2006	June 10, 2008
Last Visit Date:	July 2, 2009	January 4, 2010	December 11, 2010	January 7, 2010	February 12, 2010	June 23, 2010	August 24, 2009	August 27, 2010	May 18, 2010

Table 4. Results of paired two-sample T test of blood glucose levels at first/last participant visit

Comparing Means [Paired two-sample t-test]			
Descriptive Statistics			
VAR	**Sample size**	**Mean**	**Variance**
	9	106.92778	69.23444
	9	144.38889	275.67361
Summary			
Degrees Of Freedom	8	**Hypothesized Mean Difference**	0.E+0
Test Statistics	5.46781	**Pooled Variance**	172.45403
Two-tailed distribution			
p-level	0.0006	**t Critical Value (5%)**	2.306
One-tailed distribution			
p-level	0.0003	**t Critical Value (5%)**	1.85955
Pearson Correlation Coefficient	-0.28064		

Table 5. Results of paired two-sample T test of HbA1c levels at first/last participant visit

Comparing Means [Paired two-sample t-test]			
Descriptive Statistics			
VAR	**Sample size**	**Mean**	Variance
	9	6.92222	3.29444
	9	6.03333	0.14
Summary			
Degrees Of Freedom	8	**Hypothesized Mean Difference**	0.E+0
Test Statistics	1.45077	**Pooled Variance**	1.71722
Two-tailed distribution			
p-level	0.1849	**t Critical Value (5%)**	2.306
One-tailed distribution			
p-level	0.09245	**t Critical Value (5%)**	1.85955
Pearson Correlation Coefficient	0.04111		

Figure 1. Postulated structure and subunit composition of V-ATPase

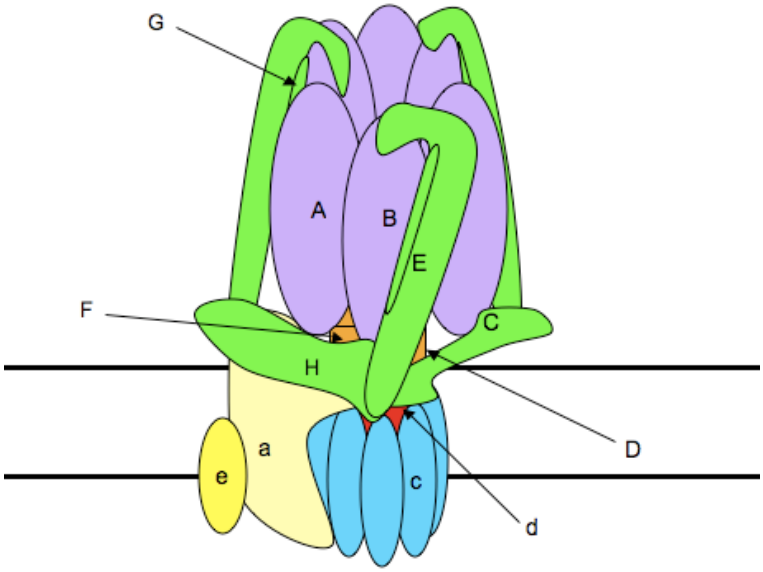

Key	
	Regulation, stabilization, ATP hydrolysis and ion translocation coupling[1]
	Catalysis, regulation, torque generation
	Axle of rotation, possible rotation
	ATP hydrolysis and ion translocation coupling
	Proton translocation
	Proton translocation
	Function unknown[2]

[1] Letters on figure represent subunits.
[2] Structure and subunit composition adapted from Muench, S.P.; Trinick, J.; Harrison, M.A., Structural divergence of the rotary ATPases. In Q Rev Biophys, 2011; pp 1-46

Figure 2. Cellular localizations and functions of V-ATPase

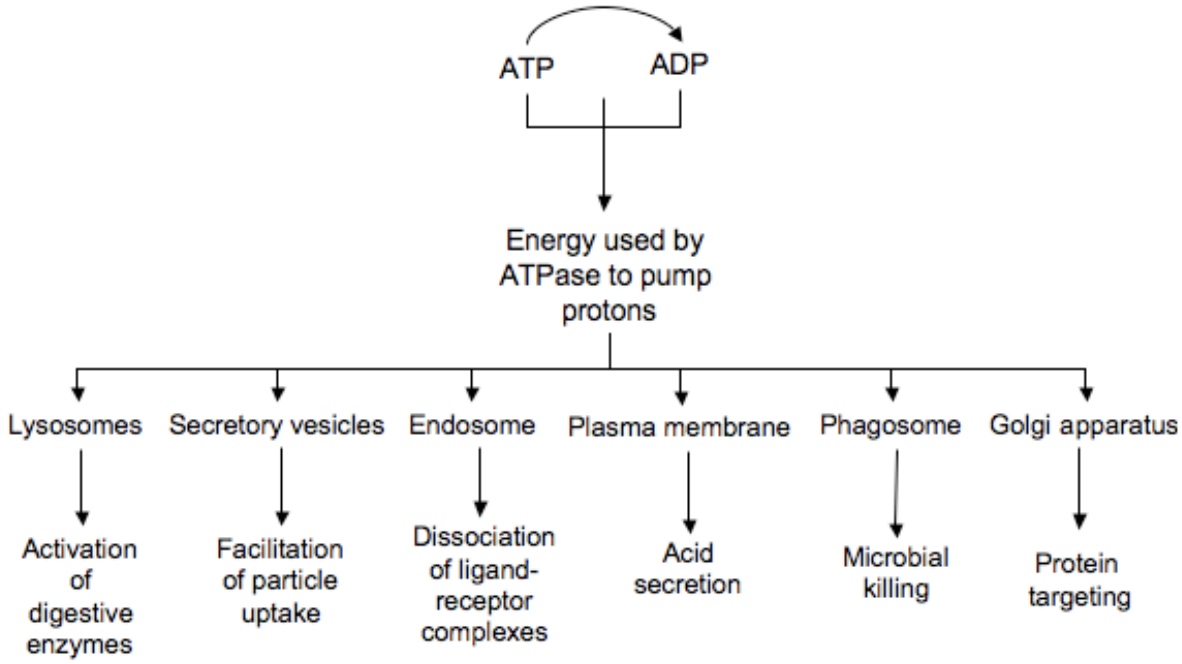

Figure 3. Gender of participants that developed diabetes

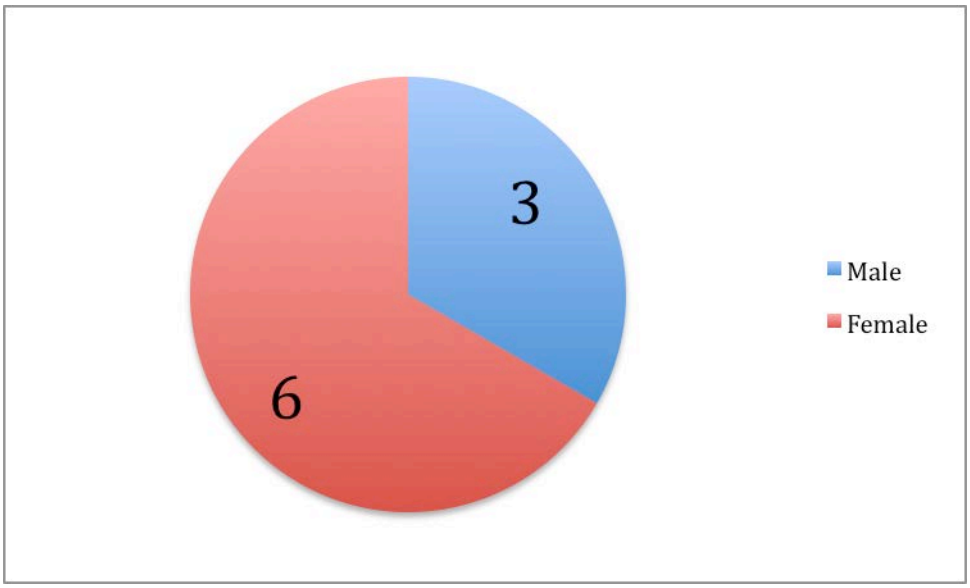

Figure 4. Age distribution of participants that developed diabetes (n = 9)

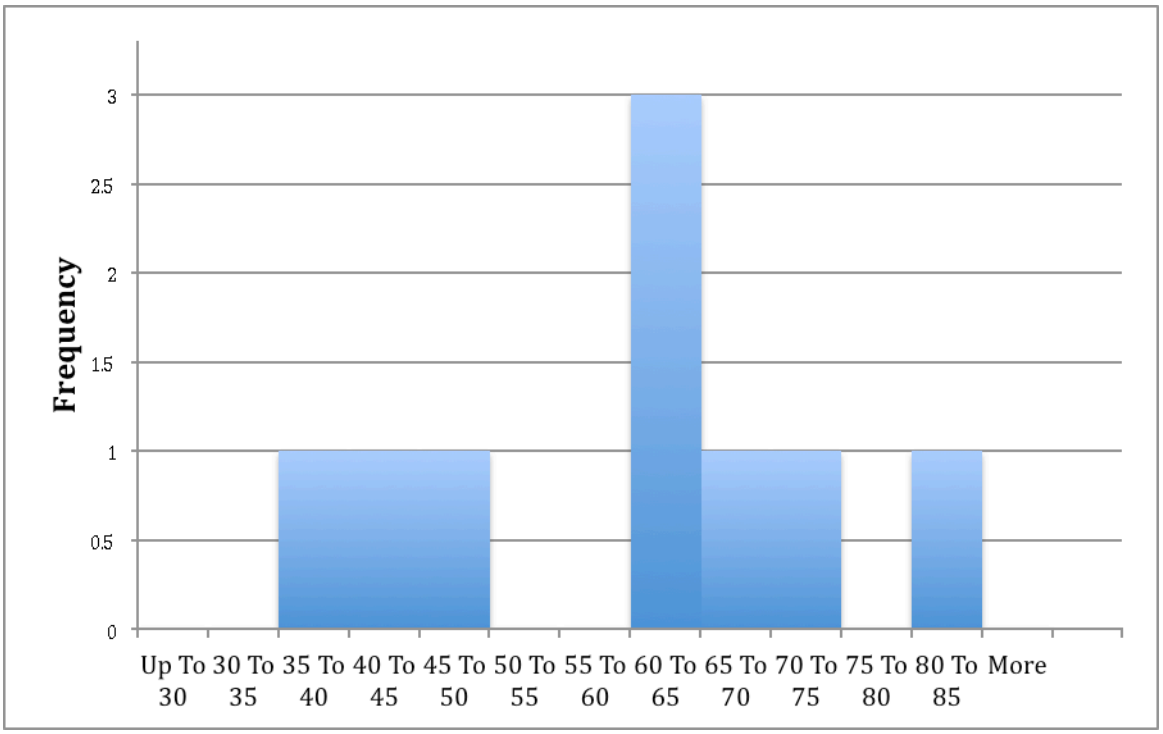

Figure 5. Weight of participants that developed diabetes: first/last visit

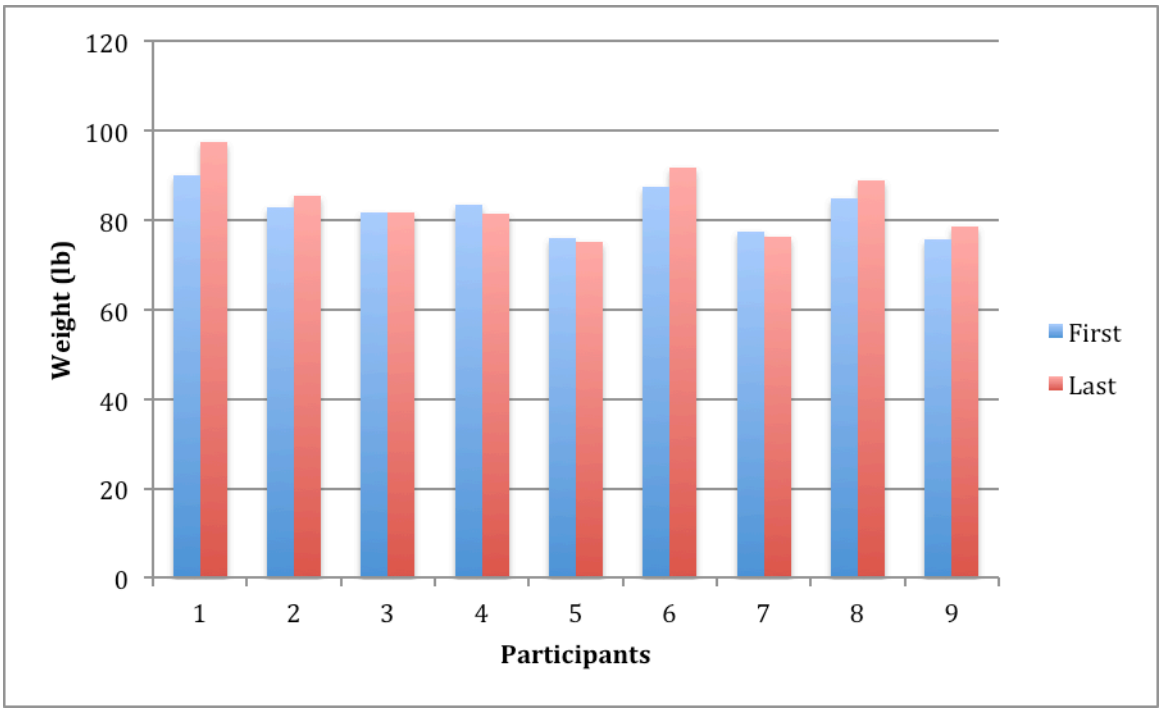

Figure 6. Triglyceride levels of participants that developed diabetes: first/last visit

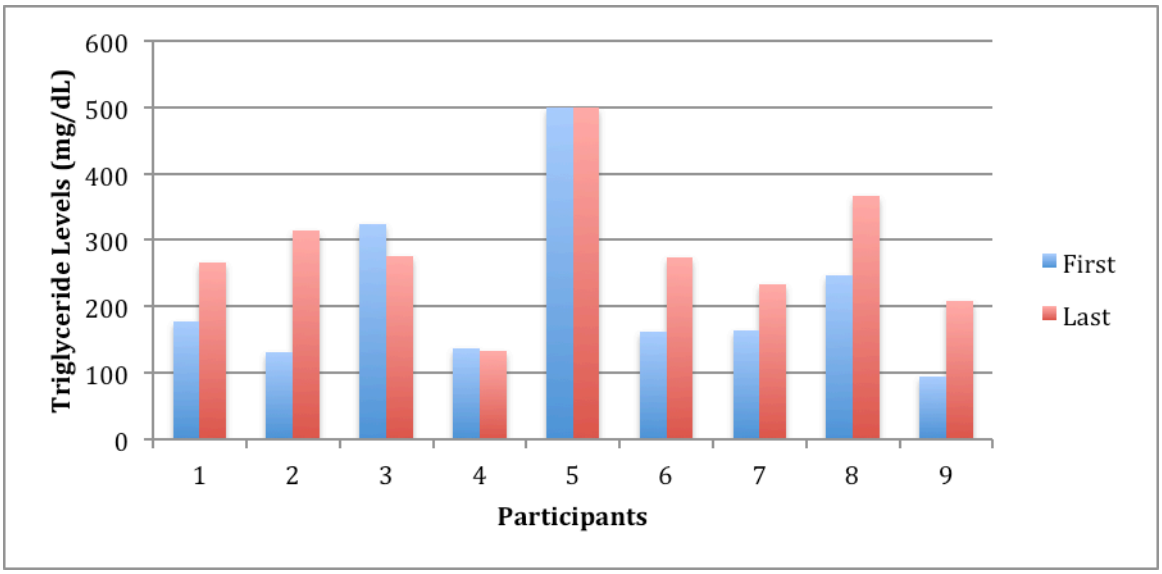

Figure 7. Cholesterol levels of participants that developed diabetes: first/last visit

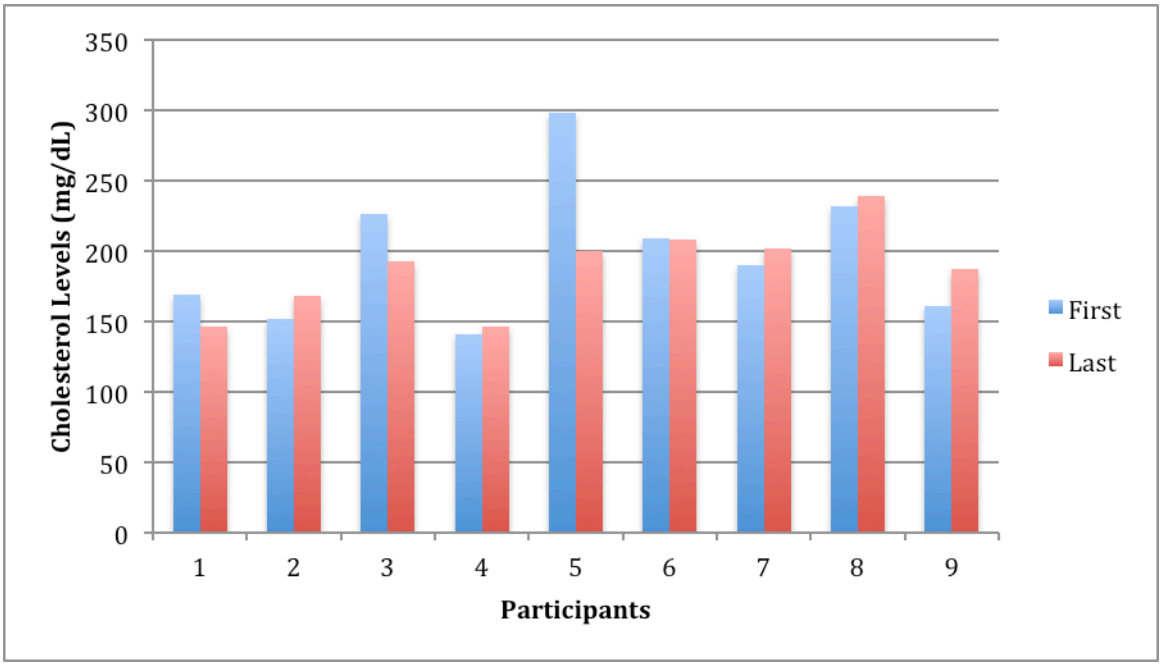

Figure 8. Glucose levels of participants that developed diabetes: first/last visit

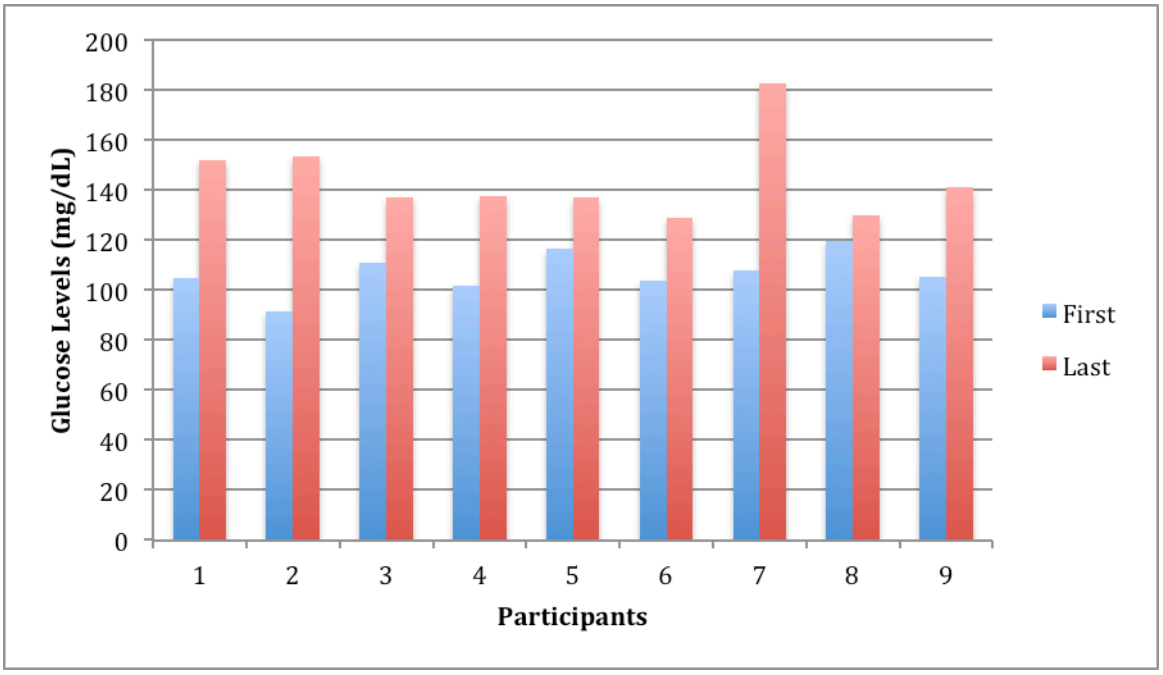

Figure 9. High-density lipoprotein cholesterol levels of participants that developed diabetes: first/last visit

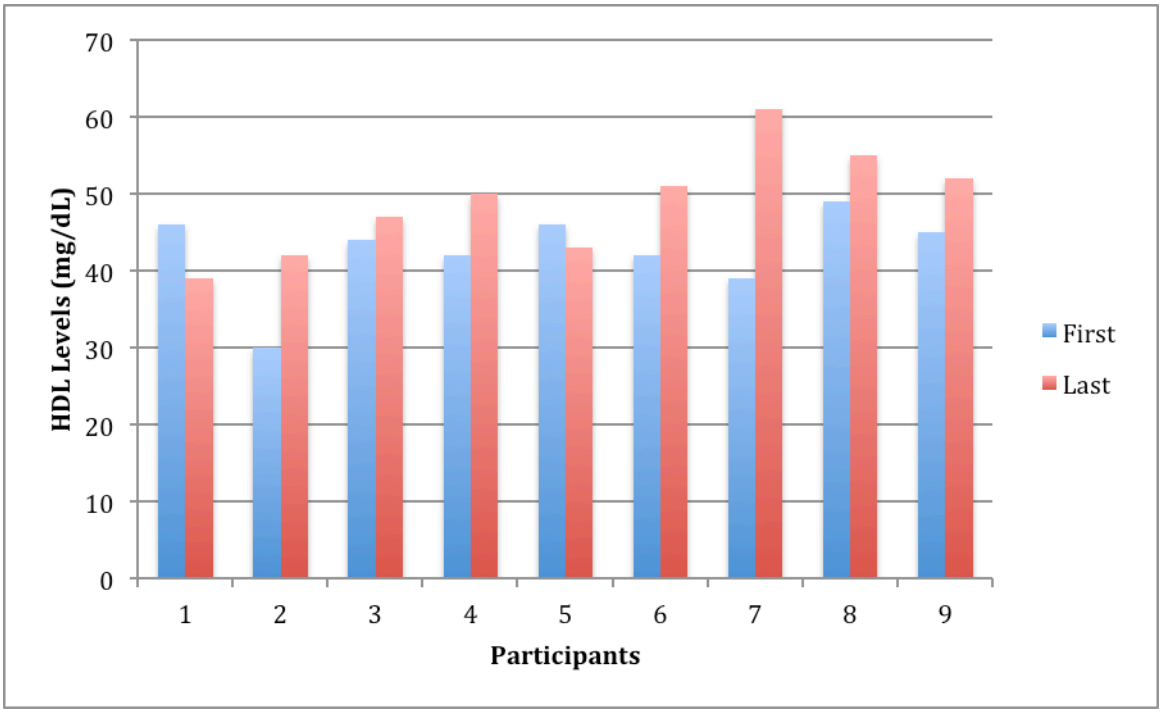

Figure 10. Low-density lipoprotein cholesterol levels of participants that developed diabetes: first/last visit

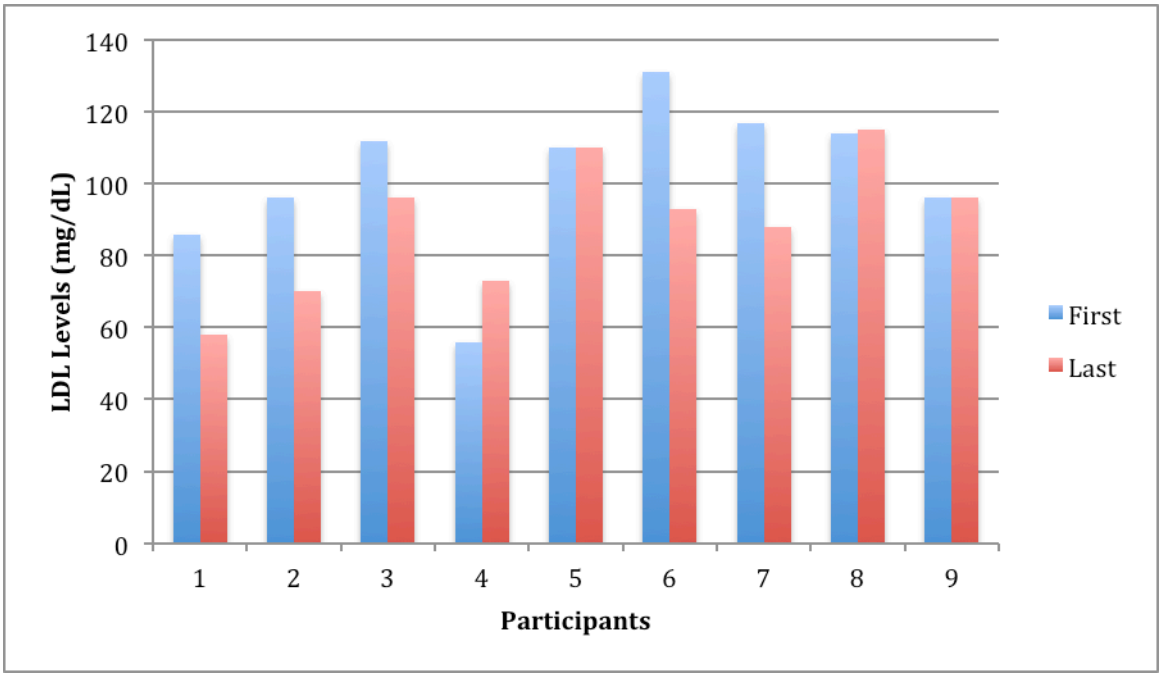

Figure 11. HbA1c levels of participants that developed diabetes: first/last visit

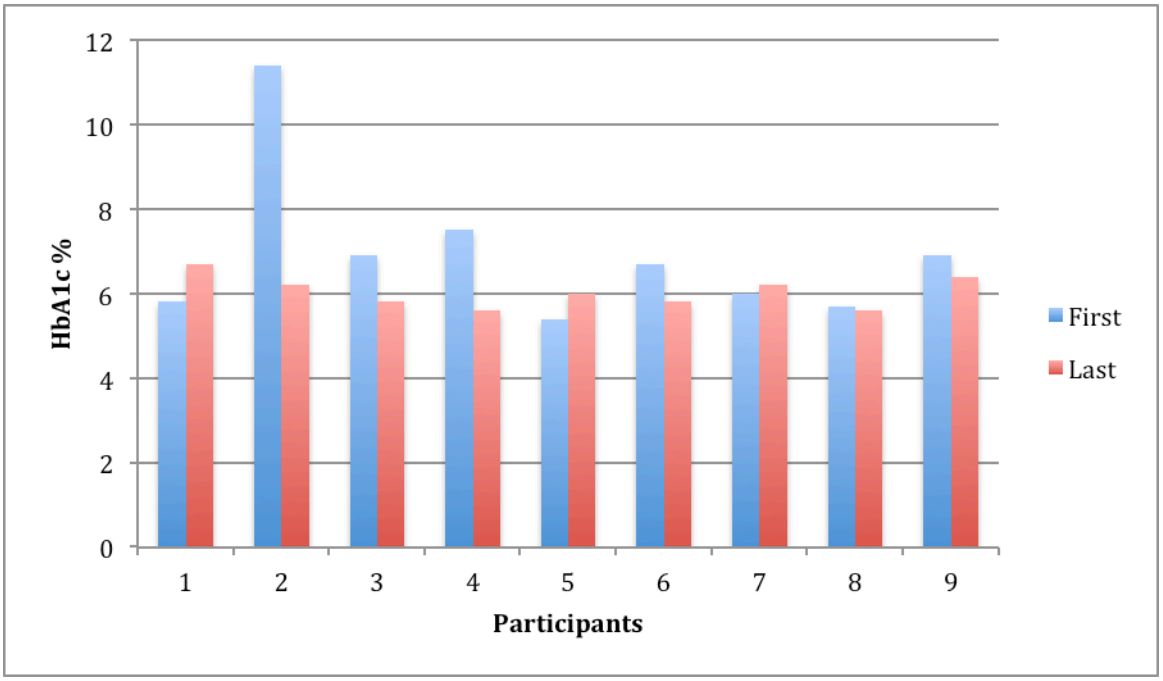

Figure 12. Expression of *ATP6V1H* in nine participants who progressed from pre-diabetes to diabetes

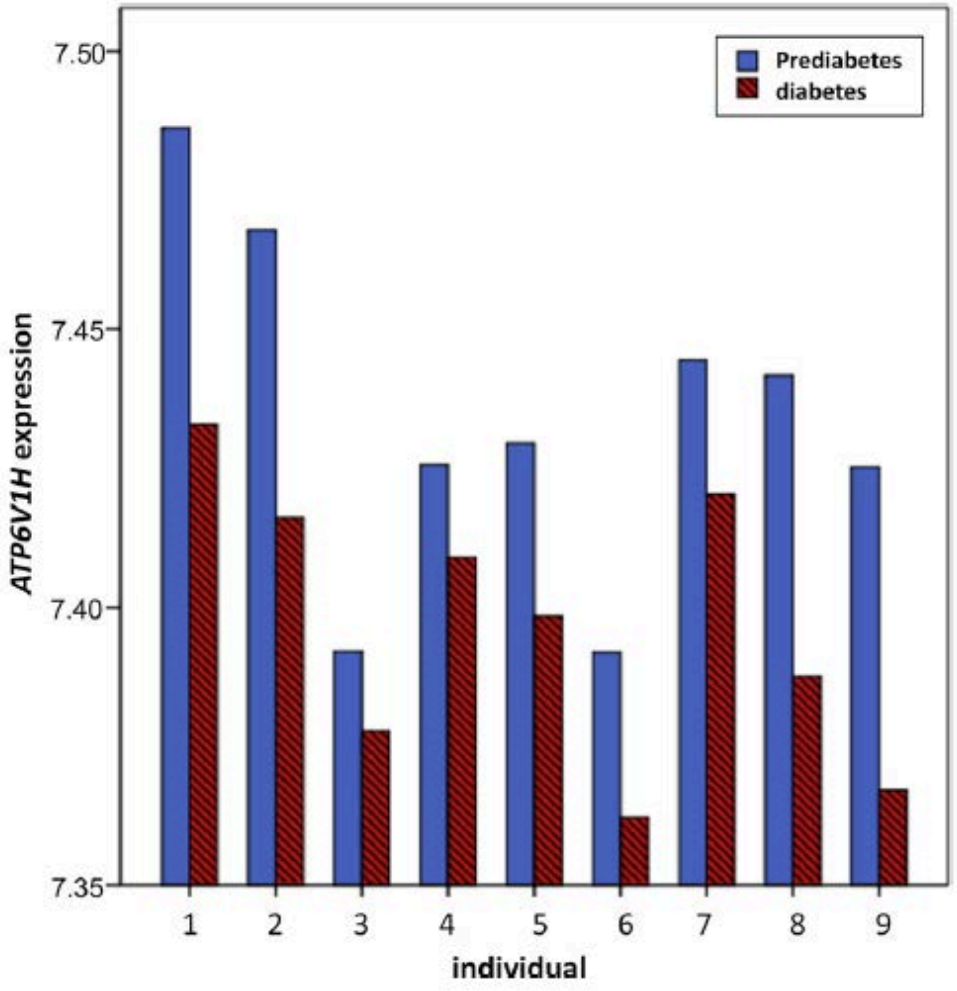

Appendices

Appendix A: Protocol for Blood RNA Purification

1. Centrifuge the PAXgene Blood RNA Tube for 10 minutes at 3000–5000 x g using a swing-out rotor.
2. Remove the supernatant by decanting or pipetting. Add 4 ml RNase-free water to the pellet, and close the tube using a fresh secondary BD Hemogard closure (supplied with the kit).
3. Vortex until the pellet is visibly dissolved, and centrifuge for 10 minutes at 3000–5000 x g using a swing-out rotor. Remove and discard the entire supernatant.
4. Add 350 µl Buffer BR1, and vortex until the pellet is visibly dissolved.
5. Pipet the sample into a 1.5 ml microcentrifuge tube. Add 300 µl Buffer BR2 and 40 µl proteinase K. Mix by vortexing for 5 seconds, and incubate for 10 minutes at 55°C using a shaker–incubator at 400–1400 rpm. After incubation, set the temperature of the shaker–incubator to 65°C (for step 20).
6. Pipet the lysate directly into a PAXgene Shredder spin column (lilac) placed in a 2 ml processing tube, and centrifuge for 3 minutes at maximum speed (but not to exceed 20,000 x g).
7. Carefully transfer the entire supernatant of the flow-through fraction to a fresh 1.5 ml microcentrifuge tube without disturbing the pellet in the processing tube.
8. Add 350 µl ethanol (96–100%). Mix by vortexing, and centrifuge briefly (1–2 seconds at 500–1000 x g) to remove drops from the inside of the tube lid.
9. Pipet 700 µl sample into the PAXgene RNA spin column (red) placed in a 2 ml processing tube, and centrifuge for 1 minute at 8000–20,000 x g. Place the spin column in a new 2 ml processing tube, and discard the old processing tube containing flow-through.
10. Pipet the remaining sample into the PAXgene RNA spin column, and centrifuge for 1 minute at 8000–20,000 x g. Place the spin column in a new 2 ml processing tube, and discard the old processing tube containing flow-through.
11. Pipet 350 µl Buffer BR3 into the PAXgene RNA spin column. Centrifuge for 1 minute at 8000–20,000 x g. Place the spin column in a new 2 ml processing tube, and discard the old processing tube containing flow-through.
12. Add 10 µl DNase I stock solution to 70 µl Buffer RDD in a 1.5 ml microcentrifuge tube. Mix by gently flicking the tube, and centrifuge briefly to collect residual liquid from the sides of the tube.
13. Pipet the DNase I incubation mix (80 µl) directly onto the PAXgene RNA spin column membrane, and place on the benchtop (20–30°C) for 15 minutes.
14. Pipet 350 µl Buffer BR3 into the PAXgene RNA spin column, and centrifuge for 1 minute at 8000–20,000 x g. Place the spin column in a new 2 ml processing tube, and discard the old processing tube containing flow-through.
15. Pipet 500 µl Buffer BR4 to the PAXgene RNA spin column, and centrifuge for 1 minute at 8000–20,000 x g. Place the spin column in a new 2 ml processing tube, and discard the old processing tube containing flow-through.
16. Add another 500 µl Buffer BR4 to the PAXgene RNA spin column. Centrifuge for 3 minutes at 8000–20,000 x g.
17. Discard the tube containing the flow-through, and place the PAXgene RNA spin column in a new 2 ml processing tube. Centrifuge for 1 minute at 8000–20,000 x g.

18. Discard the tube containing the flow-through. Place the PAXgene RNA spin column in a 1.5 ml microcentrifuge tube, and pipet 40 µl Buffer BR5 directly onto the PAXgene RNA spin column membrane. Centrifuge for 1 minute at 8000–20,000 x g to elute the RNA.
19. Repeat the elution step (step 18) as described, using 40 µl Buffer BR5 and the same microcentrifuge tube.
20. Incubate the eluate for 5 minutes at 65°C in the shaker–incubator (from step 5) without shaking. After incubation, chill immediately on ice.
21. If the RNA samples will not be used immediately, store at –20°C or –70°C. Since the RNA remains denatured after repeated freezing and thawing, it is not necessary to repeat the incubation at 65°C. If using the RNA samples in a diagnostic assay, follow the instructions supplied by the manufacturer.

Appendix B: Protocol for Microarray Analysis and Gene Expression Profiling

1. Add 10 µl 1X TE (supplied in RiboGreen kit at 20X) to B1–H1 in the plate labelled “Standard RNA”.
2. Add 20 µl ribosomal RNA to well A1.
3. Transfer 10 µl from well A1 to well B1. Pipette up and down several times.
4. Change tips. Transfer 10 µl from well B1 to well C1. Pipette up and down several times.
5. Repeat for wells C1, D1, E1, F1, and G1, changing tips each time. Do not transfer from well G1 to H1.
6. Cover the Standard RNA plate with an adhesive seal.
7. Prepare a 1:200 dilution of RiboGreen into 1X TE, using the kit supplies and a sealed 100 ml or 250 ml Nalgene bottle wrapped in aluminum foil. Use 115 µl RiboGreen and 23 ml 1X TE for 1 plate, 215 µl Ribogreen and 43 ml 1X TE for 2 plates, and so on up to 6 plates. Refer to Table 14 to identify the volumes needed to produce diluted reagent for multiple 96-well QRNA plates. For fewer than 96 RNA sam-ples, scale down the volumes.
8. Cap the foil-wrapped bottle and vortex to mix.
9. Pour the RiboGreen/1X TE dilution into a clean reagent reservoir.
10. Using a multichannel pipette, transfer 195 µl RiboGreen/1X TE dilution into each well of columns 1 and 2 of the Fluotrac plate labelled “Standard QRNA“.
11. Add 2 µl of each standard ribosomal RNA dilution from the Standard RNA plate to columns 1 and 2 of the Standard QRNA Fluotrac plate.
12. Immediately cover the plate with an adhesive aluminum seal.
13. Using a multichannel pipette, transfer 195 µl RiboGreen/1X TE dilution into each well of columns 1 and 2 of the Fluotrac plate labelled “Sample QRNA“.
14. Add 2 µl of RNA sample to all 96 wells of the Sample QRNA plate. Only the first two columns will also contain RiboGreen/1X TE dilution.
15. Immediately cover the plate with an adhesive aluminum seal.
16. Turn on the fluorometer. At the PC, open the SoftMax Pro program.
17. Load the Illumina QRNA.ppr file from the installation CD that came with your system.
18. Select Assays | Illumina | Illumina QRNA.
19. Place the Standard QRNA Fluotrac Plate into the fluorometer loading rack with well A1 in the upper left corner.
20. Click the blue arrow next to Standard RNA.
21. Click Read in the SoftMax Pro interface to begin reading the Standard QRNA Plate.
22. When the software finishes reading the data, remove the plate from the drawer.
23. Click the blue arrow next to Standard Curve to view the standard curve graph.
24. If the standard curve is acceptable, continue with the sample plate. Otherwise, click Standard Curve again.
25. Place the first Sample QRNA plate in the fluorometer with well A1 in the upper left corner.
26. Click the blue arrow next to QRNA#1 and click Read.
27. When the software finishes reading the plate, remove the plate from the drawer.

28. Repeat steps 10 through 12 to quantitate all Sample QRNA plates.
29. Once all plates have been read, click File | Save to save the output data file (*.pda).
30. When you have saved the *.pda file, click File | Import/Export | Export and export the file as a *.txt file. You can open the *.txt file in Microsoft Excel for data analysis.

Hybridize BeadChip

1. Preheat the cRNA sample tube at 65°C for 5 minutes.
2. Vortex the cRNA sample tube, then pulse centrifuge the tube at 250 xg.
3. Allow the cRNA sample tube to cool to room temperature, then proceed as soon as the tube has cooled.
4. Using a single-channel precision pipette, add the appropriate volume from each cRNA sample tube into each hybridization tube.
5. Using a single-channel precision pipette, add the appropriate volume of RNase-free water into each cRNA sample tube.
6. Using a single-channel precision pipette, add the appropriate volume of HYB into each cRNA sample tube.
7. Assemble the Hyb Chambers
    a. Place the following items on the bench top:
        i. BeadChip Hyb Chamber (1 per 4 BeadChips)
        ii. BeadChip Hyb Chamber gasket (1 per Hyb Chamber)
        iii. BeadChip Hyb Chamber inserts (4 per Hyb Chamber
    b. Place the Hyb Chamber Gasket into the Hyb Chamber as follows:
        i. Match the wider edge of the Hyb Chamber gasket to the barcode-ridge side of the Hyb Chamber.
        ii. Lay the gasket into the Hyb Chamber, and then press it down all around.
        iii. Make sure the Hyb Chamber gasket is properly seated.
    c. Add 200 µl HCB into the eight humidifying buffer reservoirs in the Hyb Chamber. If you are hybridizing fewer than four BeadChips, only fill the reservoirs of sections that will contain BeadChips.
    d. Close and lock the BeadChip Hyb Chamber lid.
        i. Seat the lid securely on the bottom plate.
        ii. Snap two clamps shut, diagonally across from each other.
        iii. Snap the other two clamps.
    e. Leave the closed Hyb Chamber on the bench at room temperature until the BeadChips are loaded with the DNA sample.
8. Prepare BeadChips for hybridization
    a. Remove all the BeadChips from their packages.
    b. Place each BeadChip in a Hyb Chamber Insert, orienting the barcode end so that it matches the barcode symbol on the Hyb Chamber Insert.
9. Load sample.
    a. Using a single-channel precision pipette, add the appropriate volume of DNA sample onto the center of each inlet port.

b. Visually inspect all sections. Ensure sample covers all of the sections of the stripe. Record any sections that are not covered. Some residual sample may still remain in the inlet port. This is normal.
c. Open the Hyb Chamber.
d. Load 4 Hyb Chamber Inserts containing sample-laden BeadChips into each Hyb Chamber.
e. Position the barcode end over the ridges indicated on the Hyb Chamber and ensure the inserts are securely seated.

10. Close and lock the BeadChip Hyb Chamber lid.
    a. Seat the lid securely on the bottom plate.
    b. Snap two clamps shut, diagonally across from each other.
    c. Snap the other two clamps.
    d. Check to ensure that the Hyb Chamber is completely closed, as any gap in the seal will result in evaporation during hybridization and will compromise analytical data.
11. Place the Hyb Chamber into the 58°C Illumina Hybridization Oven so that the clamps face the left and right sides of the oven. The Illumina logo on top of the Hyb Chamber should face you.
12. (Optional) Start the rocker at speed 5. Turn on the switch just above the power switch.
13. Close the Illumina Hybridization Oven door.
14. Incubate the BeadChips for at least 14 hours but no more than 20 hours at 58°C.
15. Update the lab tracking form with the start and stop times.
16. Prepare High-Temp Wash Buffer
    a. In preparation for the next day's washes, prepare 1X High-Temp Wash buffer from the 10X stock by adding 50 ml 10x High-Temp Wash buffer to 450 ml RNAse-free water.
    b. Place the Hybex Waterbath insert into the Hybex Heating Base.
    c. Add 500 ml prepared 1X High-Temp Wash buffer to the Hybex Waterbath insert.
    d. Set the Hybex Heating Base temperature to 55°C.
    e. Close the Hybex Heating Base lid and leave the High Temp Wash buffer to warm overnight.
    f. Proceed to *Wash BeadChip* on page 53 the next day.

Wash BeadChip

1. Remove the Hyb Chamber from the oven and place it on the lab bench. Disassemble the chamber.
2. Using powder-free gloved hands, remove all BeadChips from the Hyb Chamber and submerge them face up at the bottom of the beaker.
3. Using powder-free gloved hands, remove the coverseal from the first BeadChip under the buffer. This may require significant force, due to the strength of the adhesive. Ensure that the entire BeadChip remains submerged during removal.
4. Using tweezers or powder-free gloved hands, transfer the BeadChip to the slide rack submerged in the staining dish containing 250 ml Wash E1BC solution. This is the

staging area to hold the BeadChips until all coverseals have been removed under the buffer.
5. Repeat steps 3 and 4 for all BeadChips from the same Hyb Chamber.
6. Using the slide rack handle, transfer the rack into the Hybex Waterbath insert containing High-Temp Wash buffer that was prepared the previous day (see *Prepare High-Temp Wash Buffer* on page 47).
7. Close the Hybex lid.
8. Incubate static for 10 minutes.
9. After the 10-minute incubation in High-Temp Wash buffer is complete, immediately transfer the slide rack back into a staining dish containing 250 ml fresh Wash E1BC buffer.
10. Using the slide rack handle, plunge the rack in and out of the solution 5–10 times.
11. Set the orbital shaker to medium-low.
12. Place the staining dish on the orbital shaker and shake at room temperature for 5 minutes. Shake at as high a speed as possible without allowing the solution to splash out of the staining dish.
13. Transfer the rack to a new staining dish containing 250 ml fresh 100% Ethanol.
14. Using the slide rack handle, plunge the rack in and out of the solution 5–10 times.
15. Place the staining dish on the orbital shaker and shake at room temperature for 10 minutes.
16. Transfer the rack to the same staining dish containing 250 ml Wash E1BC buffer.
17. Using the slide rack handle, plunge the rack in and out of the solution 5–10 times.
18. Place the staining dish on the orbital shaker and shake at room temperature for 2 minutes.
19. Place the BeadChip wash tray on the rocker mixer.
20. Add 4 ml Block E1 buffer to the Wash Tray.
21. Using tweezers, transfer the BeadChip face up into the BeadChip wash tray. The barcode should be at the well end. Use the well at the end of the wash tray to grip the BeadChip.
22. Pick the wash tray up and gently tilt it manually to ensure the BeadChip is completely covered with buffer.
23. Place the wash tray back onto the rocker platform and rock at medium speed for 10 minutes.
24. Clean the Hyb Chambers:
    a. Remove the rubber gaskets from the Hyb Chambers.
    b. Rinse all Hyb Chamber components with DI water.
    c. Thoroughly rinse the eight humidifying buffer reservoirs.
25. Discard unused reagents in accordance with facility standards.
26. Proceed to *Detect Signal*.

Detect Signal

1. Using tweezers, grasp the BeadChip at the barcode end via the well in the blocker wash tray.
2. Transfer the BeadChip to the wash tray containing Cy3-Streptavidin. Place it flat with the barcode near the tweezer well.

3. Pick the wash tray up and gently tilt it manually to ensure the BeadChip is completely covered with buffer.
4. Cover the wash tray with the flat lid provided.
5. Place the tray on the rocker mixer.
6. Rock the BeadChip on medium for 10 minutes.
7. Add 250 ml Wash E1BC into a clean staining dish with a slide rack.
8. Using tweezers, grasp the BeadChip at the barcode end and remove it from the wash tray.
9. Transfer the BeadChip into the slide rack submerged in the staining dish. Immediately submerge the BeadChip into the Wash E1BC.
10. Using the slide rack handle, plunge the rack in and out of the solution 5 times.
11. Set the orbital shaker to medium-low.
12. Ensure the BeadChip is completely submerged in the Wash E1BC.
13. Place the staining dish on the orbital shaker and shake at room temperature for 5 minutes.
14. Set the centrifuge to 1,400 rpm at room temperature for 4 minutes.
15. Place clean paper towels on the centrifuge microtiter plate holders to absorb excess solution.
16. Fill the staining dish balance slide rack with an equivalent number of standard glass microscope slides.
17. Using powder-free gloved hands, quickly pull the slide holder out of the Wash E1BC.
18. Transfer the rack of BeadChips from the staining dish to the centrifuge, close the door, and press Start.
19. Transfer the rack of BeadChips from the staining dish to the centrifuge. Centrifuge at 1,400 rpm at room temperature for 4 minutes.
20. Once the BeadChips are dry, store them in a dark, ozone-free environment until ready to scan.
21. Discard unused reagents in accordance with facility standards.

Image BeadChip on the BeadArray Reader

1. Open the BeadScan software.
2. Log in and click Scan to display the Welcome window.
3. From the Docking Fixture dropdown list, select BeadChip.
4. Check the Data Repository path and the Decode Map path in the Settings area.
    a. The Data Repository indicates where the BeadArray Reader stores the images created during the scan. The default path is C:\ImageData.
    b. The Decode Map Path points to the location where you will copy the files from the BeadChip CD. The default path is C:\DecodeData.
5. If either path in the previous step is not correct, follow these steps:
    a. Click Edit to open the Options dialog box.
    b. Click Browse to navigate to and select the Data Repository path and the Decode Map path.
    c. Select or clear the Save Compressed Images check box. Compressed images use the *.jpg format. Uncompressed images use the *.tiff format and may be 75 MB or more.
    d. After changing settings, click either Save for This Scan or Save for All Scans.

6. For each BeadChip, download the decode content from iCom or copy the contents of the DVD provided with the BeadChip (if purchased) into the Decode folder. The folder name should be the BeadChip barcode (for example, 4264011131).
7. For each BeadChip:
    a. Place the BeadChip into the BeadArray Reader tray.
    b. Using the hand-held barcode scanner, scan the BeadChip barcode. The barcode appears on the screen in the position corresponding to the BeadChip position in the tray. The Sentrix Type column should say “BeadChip 8x1” and the Scan Settings should say “Direct Hyb”.
    c. If either the Sentrix Type or Scan Settings are not correct, click Browse (...) to open the Select Scan Settings dialog box.
    d. Select Direct Hyb and click Select.
8. Make sure that the BeadChips are properly seated in the BeadArray Reader tray.
9. Click Scan.
10. Click OK on the Scan Completed message to view the next screen.
11. Click Done in the Review pane.
12. When the application returns to the Welcome screen, click Open Tray. The BeadArray Reader tray, loaded with the scanned BeadChips, will eject.
13. Remove the BeadChips from the tray.
14. Do one of the following:
    a. If you have more BeadChips to scan, repeat the scanning process.
    b. If this is the last use of the day:
        i. Wipe the BeadArray Reader tray with a lint-free, absorbent towel. Pay particular attention to the tray edges where reagent may have wicked out.
        ii. Close the tray.
        iii. Turn the power switch at the back of the scanner to the OFF position.
        iv. Shut down the BeadArray Reader BeadScan software. To exit, right-click near the Illumina logo and click Exit.

AUTHOR BIOGRAPHY

Melanie Molina is graduating as a Dean's Honored Graduate and a member of Phi Beta Kappa from The University of Texas at Austin with a B.A. in Hispanic Studies (departmental honors) and a B.S. in Honors Biology in May of 2012. Melanie was born and raised in Austin, however, both of her parents share strong roots in the southernmost part of Texas known as "the Valley," and it is partly for that reason that Melanie chose to conduct her research in Brownsville.

At UT, Melanie was actively involved in Global Medical Training and the Hispanic Health Professions Organization as the public relations officer for both organizations. With GMT, she traveled to Nicaragua, Panama and the Dominican Republic on medical missions. Having been inspired by the health disparities she experienced in those countries firsthand, she developed a passion for public health and seized the opportunity to conduct an internship with the Texas Department of State Health Services. This internship led her to another opportunity in Brownsville, working under the guidance of Dr. Susan Fisher-Hoch and Dr. Joseph McCormick at The University of Texas School of Public Health.

In the fall, Melanie will be attending Harvard Medical School. She plans to earn a Masters of Public Health in addition to her M.D. Ultimately, she hopes to implement the knowledge she gains in medicine and public health abroad, in order to improve the health disparities in Third World Latin-American countries.